NEW STRATEGIES FOR KINETIC ENERGY DENSITY FUNCTIONALS

NEW STRATEGIES FOR KINETIC ENERGY DENSITY FUNCTIONALS

By XIAOMIN HUANG, M. Sc.

A Thesis Submitted to the School of Graduate Studies in Partial Fulfilment of the Requirements for the Degree Master of Science

McMaster University MASTER of SCIENCE (2020)

(Chemistry and Chemical Biology)

Hamilton, Ontario, Canada

TITLE:	New Strategies for Kinetic Energy Density Functionals
AUTHOR:	Xiaomin Huang (M. Sc. Chemistry Universidad Nacional Autónoma de México)
SUPERVISOR:	Professor Dr. Paul W. Ayers
NUMBER OF PAGES:	*xi*, 71

Abstract

Orbital-free density functional theory requires accurate approximations for the noninteracting kinetic energy as a functional of the ground-state electron density. For explicit functionals in real space, it has proved difficult to supersede the quality of the gradient expansion, truncated at second order. This is partly because the gradient expansion diverges for atomic and molecular densities. In an effort to include information about higher-order terms in the gradient expansion but avoid divergences, we consider resummations for the series using Padé approximants and Meijer-G functions. To regularize terms that appear in the denominator, we consider various damping functions, which introduces parameter(s) that can be fit to atomic data. These results improve upon the second-order truncation, but do not achieve the exquisite accuracy that would be required for practical orbital-free density-functional theory calculations.

Acknowledgements

I want to thank Dr. Paul Ayers for all his guidance and support for the past 3 years. He always gave me freedom to explore my scientific interests by getting me involved in different lines of research. He offered lots of opportunities to acquire new skills, such as teaching, public speaking, and management. More importantly, I am grateful that Paul supported my decision to defend this work. I completed this research thanks to Paul's insight and supervision throughout the program.

I would also like to thank everyone from the Ayers Group, specially, Cristina González Espinoza for taking the time to explain how to use HORTON[1]. Thanks to Derrick Yang and David Kim for always helping me with every struggle I had. Thanks to Kumru Dikmenli and Jennifer H. Garner for keeping me motivated. Thanks to everyone who contributed to the HORTON package. This work would take much longer without it.

Finally, I want to thank all my friends and family that always encouraged me to achieve my goals and for all their emotional support. Your motivation helped me push myself to move forward.

Contents

List of Figures

List of Tables

Declaration of Academic Achievement

Dr. Paul Ayers provided the main ideas for putting this work together. The author wrote a program that calculates the kinetic energy of a chemical system given a functional approximation. The code utilizes the Ayers Group's software package for electronic calculations named HORTON [1]. Several kinetic energy density functional approximations were tested thoroughly using a small set of atoms and molecules. The thesis is comprised of unpublished content.

Chapter 1

Introduction

When modelling chemical phenomena computationally, one is limited primarily by one's computational resources. For example, if one wishes to simulate the movements of large molecules on significant timescales, one typically uses classical molecular mechanics methods. These methods are fast enough to treat systems with millions of atoms, or somewhat smaller molecules on the millisecond timescale because they directly encode the energy using a classical potential energy function, which is typically expressed in terms of bond-stretching, angle-bending, bond-torsion, and nonbonded terms.[3]. For chemical reactions, however, one needs to be able to not only stretch and bend, but break, chemical bonds [4]. Classical force fields do not suffice here.

To describe the dynamics of chemical reactions, one can use ab initio molecular dynamics (AIMD), where the forces on atoms are determined by solving the electronic Schrödinger equation.[5]. This allows bond-breaking to be con-

sidered but typically only systems with hundreds of atoms can be treated, and even then, only for a few picoseconds.[4].

This motivates work on improving the speed by which atomic forces can be evaluated from quantum mechanics. For most applications, the current state-of-the-art is Kohn-Sham density functional theory (KS-DFT). KS-DFT is not as costly as more traditional wavefunction-based methods, but achieves similar performance. For studying systems with hundreds of atoms at nonzero temperature, or thousands of atoms at zero temperature, KS-DFT is not routinely practical. The temperature dependence can be understood because as the temperature increases, additional electronic states are required and the atoms move more rapidly, necessitating solving for more electronic states and using smaller time-steps.[6]. In addition, the cost of KS-DFT methods naïvely increases as $O(N^3)$. While linear-scaling KS-DFT methods exist, their efficiency is mostly realized for very large systems.

The poor computational scaling of Kohn-Sham DFT is determined by the need to solve, either explicitly or implicitly, for the orbitals of each electron in the system.[7]. It has been known since the 1920's that this cost can be reduced by using orbital-free methods. In orbital-free density-functional theory (OF-DFT), the electron density is determined directly, without any consideration of the electronic orbitals. Low-cost calculations are easily realized and, in fact, for OF-DFT the limiting cost becomes evaluating long-range Coulomb interactions, which is exactly the same operation that limits the effectiveness of classical molecular dynamics methods. Despite its great promise, however,

OF-DFT is not commonly used. This is because it is difficult to determine the energy as a functional of the electron density without any reference to electronic orbitals.[8].

The energy in density functional theory is commonly decomposed into the noninteracting kinetic energy (which is exactly computed from orbitals in KS-DFT), the classical Coulomb attraction of the electrons to the nuclei, the classical Coulomb repulsion of the electrons for each other, and the exchange-correlation term, which captures the effects of the Pauli principle (on the potential energy) and electron correlation (on both the kinetic and potential energy). The classical electrostatic terms can be exactly expressed as functionals of the electron density, and accurate approximations to the exchange-correlation energy have been developed over the last 30 years.[9]. Accurate approximate expressions for the noninteracting kinetic energy as an explicit functional of the electron density, on the other hand, are sorely lacking.[10, 11].

There are many strategies for developing kinetic energy density functionals, and in this work we will focus on strategies in real space. (Approximations in reciprocal space are also possible, and often perform a bit better, but have their attendant difficulties also.[12]) The starting point for most calculations is the Thomas-Fermi functional.[13, 14, 15]. The Thomas-Fermi functional is exact for the uniform electron gas (also called jellium), where the electron density is the same everywhere and the relative error in the Thomas-Fermi functional for neutral atoms decreases to zero as the atomic number increases to infinity. Unfortunately, the Thomas-Fermi functional is inaccurate both

quantitatively and qualitatively. In particular, the Teller nonbinding theorem indicates that Thomas-Fermi OF-DFT predicts that no stable diatomic molecules exist.[16]. The electron density in atoms and molecules is far from uniform, which suggests that one might improve the Thomas-Fermi method using perturbation theory in the norm of the gradient of the density: that is, one might consider, perturbatively, the effect of inhomogeneity in the electron density. This leads to the gradient expansion.[10, 17, 18, 19, 20]. The odd-order terms in the gradient expansion vanish uniformly, so it was a relief to observe that the second-order term in the gradient expansion approximation (GEA2) was already a great improvement over the Thomas-Fermi functional in most cases. Unfortunately, higher-order terms in the expansion do not improve the situation.[21]. In fact, the expansion diverges for atomic and molecular densities and even specific terms in the expansion diverge.[19, 22]. This result is perhaps not that surprising as atomic and molecular electron densities are highly inhomogeneous, but it is nonetheless discouraging, since it makes it seem very difficult to ever build a systematic mathematical approach to more accurate kinetic energy functionals.

But are matters this hopeless? There are numerous methods—some recently developed—for resumming divergent series. For example, Sergeev *et al.* [23, 24] demonstrated that using a Padé approximant to resum the gradient expansion gives some improvement in estimating the kinetic energy. Padé approximants are not the most general way to resum a series, however, because they assume that the underlying function is a rational function. A traditional (m, n) Padé approximant, for example, is a poor choice for a series that di-

verges due to a branch point. Recently, Mera *et al.* [25, 26] showed that a Meijer-G function is more appropriate for such series, and the convergence of a hypergeometric resummation happens at low orders.

The primary goal of this thesis is to explore these hyperasymptotic resummation techniques for the gradient expansion of the noninteracting kinetic energy functional in Kohn-Sham DFT. Chapter 2 reviews the main concepts of resummation and DFT. Chapter 3 contains computational details and discusses the various functionals we considered. Finally, our results are presented, and summarized, in chapters 4 and 5.

Chapter 2

Theoretical Framework

2.1 Summation of Divergent Series

Series are often used to approximate functions that are difficult to evaluate directly. For example, when evaluating the electronic energy of an N-particle system, the exact energy can only be evaluated in the limit where the electron-electron interactions vanish. However, by using the value of the energy and its derivatives with respect to electron-electron interaction strength in this limit, one can form a Taylor series. Evaluating this Taylor series term-by-term, and truncating the expansion at some order, is the Möller-Plesset perturbation theory method [27].

2.1.1 Series Convergence

The summation of a Taylor series may converge to a certain value or diverge. A series is convergent when the Cauchy criterion is met [28, 29]. Given a series $\sum_{n=0}^{\infty} a_n$, it converges if its partial sums are a Cauchy sequence. That is, defining $s_j = \sum_{n=0}^{j} a_n$, a series converges if for every $\epsilon > 0$, there exists a number N, such that for all $i > N$ and $j > N$, $|s_j - s_i| < \epsilon$. One can do a preliminary analysis by checking if the terms, a_n, ultimately go to zero. This test does not guarantee convergence (consider the case $a_n = n^{-p}$ with $0 < p \leq 1$) but if it fails, then the series diverges. A better test in the same spirit is the D'Alembert ratio test of successive terms. [29]

$$\rho = \lim_{n \to \infty} \frac{a_{n+1}}{a_n} \tag{2.1}$$

If $\rho < 1$ the series converges, if $\rho > 1$, it diverges and if $\rho = 1$ then it is undetermined. Many other tests can be used, such as the quotient test, comparison test, root test, and integral test.

Establishing the convergence of a series is helpful, but perturbation theory is only practical when the series is rapidly convergent. In cases where a series is divergent, sometimes useful results can be obtained by identifying the optimal truncation, as there sometimes a low-order truncation can provide usefully accurate results.[30]. Clearly the fewer terms need to be evaluated to obtain a sufficiently accurate approximation, the more practically useful series expansion is.

Asymptotic analysis is useful when studying divergent series. A Taylor series is said to be asymptotic to a certain function $f(x)$, if, for a certain N and value of $x \to L$, [30]

$$\left| f(x) - \sum_{n=0}^{N} z_n x^n \right| \sim \mathrm{o}\left(x^{N+1}\right), \tag{2.2}$$

meaning that the error in the function evaluated at x and the truncated sum of the series up to the N^{th} term has an error of the same order as the first neglected term in the series. Every convergent series is asymptotic but not every asymptotic series is divergent. One well-known asymptotic series is Stirling's approximation for the logarithm of the Gamma function,

$$\ln \Gamma(x) \sim x \ln x - x + \frac{1}{2} \ln\left(\frac{2\pi}{x}\right) + \sum_{n=1}^{N-1} \frac{B_{2n}}{2n(2n-1)x^{2n-1}} \tag{2.3}$$

For example, for a fixed value of x, the error with respect to $\ln \Gamma(x)$ reaches an x-dependant minimum after a certain N and grows indefinitely afterwards.

A series is supersaymptotic if it is optimally-truncated, usually meaning that the chosen N yields the minimum error for a given x. Generally the error is smaller than any term in the expansion (e.g., proportional to $\exp(-\frac{\text{constant}}{x})$). The optimal truncation often occurs for the smallest term in the expansion, and typically the optimal N often increases as x increases (e.g., $N_{\text{opt}} \propto x^{-1}$).[31].

A hyperasymptotic approximation uses a resummation technique. That is, it adds terms to a superasymptotic expansion based on the asymptotic series, giving a lower error than the superasymptotic expansion by itself.[31]. The

main objective of hyperasymptotics is to reduce error, and also the number of terms needed for it. Convergence acceleration can also be achieved using sequence transformations, meaning a new sequence with better numerical properties is considered. Convergence of the sum of the new sequence is not guaranteed, and trial and error is often required. For example, the simplest transformation is a linear scaling using a set of weights. The advantage is that they resulting series converges to the same limit, but it is no more efficient. Nonlinear transformations are less straightforward, but they can be very powerful if used correctly. The disadvantage is that the convergence is not guaranteed and, because of the complicated form, the properties of the transformations are not always completely understood.[32].

Resummation techniques are especially important for divergent series. In favourable cases, a resummation technique can estimate the original function that gave rise to the asymptotic or even wholly divergent series. One popular technique is Padé approximants, where terms in the Taylor series reproduced by a rational function with polynomials as the denominator and numerator.[30]. Padé approximants work well for series which diverge due to poles in the complex plane. For example, the Padé approximant $p(x) = (1+x^2)^{-1}$ is an exact resummation of the divergent series $s(x) = 1 - x^2 + x^4 - x^6 + \cdots$.

The Borel method is another popular resummation technique. In the Borel method, one first performs the Borel transformation of the series, wherein each term in the series is divided by $n!$. The series is then summed (perhaps

approximately) in the Borel plane, and then transformed back by a Laplace transform. For example, appling the Borel transform to the divergent series

$$Z(x) = 1 - x^2 + x^4 - x^6 + \cdots \tag{2.4}$$

$$B(t) = 1 - \tfrac{1}{2!}t^2 + \tfrac{1}{4!}t^4 - \tfrac{1}{6!}t^6 + \cdots \tag{2.5}$$

which we can recognize as

$$B(t) = cos(t) \tag{2.6}$$

The re-summed series is

$$Z_B(x) = \int_0^\infty \cos(xt)e^{-t}dt \tag{2.7}$$

$$= (1 + x^2)^{-1} \tag{2.8}$$

The link to the Laplace transform may not be entirely clear, but notice that we can rearrange the transformation from the Borel plane as:

$$Z_B(x) = \int_0^\infty B(xt)e^{-t}dt \tag{2.9}$$

$$= x^{-1}\int_0^\infty B(u)e^{-u/x}du \tag{2.10}$$

$$Z_B(y^{-1}) = y\int_0^\infty B(xt)e^{-yu}dt \tag{2.11}$$

Borel transformation is effective when it is possible to resum the transformed series in some way, preferably a way such that the Laplace transform can be evaluated analytically. A common technique is to resum the series in the

Borel plane using Padé approximants. However, it is often helpful to use a more general form, which can model transcendental functionals also. In Ref. [25, 26], a hypergeometric resummation was considered, which results in a Meijer-G approximant. This method is advantageous because the Laplace transform of hypergeometric functions is known, and because hypergeometric functions are extremely flexible, and can model polynomials, rational functions, and transcendental functions. One conclusion from the examples above is that if the series expansion corresponds to a function, and that function is used to model the resummation of that expansion, then the resummation is exact. I.e., the divergent Taylor series of a rational function is exactly resummed by a Padé approximant. Similarly, given a divergent series that corresponds to the Meijer-G function, a Meijer-G resummation will be exact. More generally, if a divergent series corresponds to a function that can be accurately fit by a Padé approximant or a Meijer-G function, then resummations based on those functions will be exact.

2.1.2 Padé approximants

Padé approximants are commonly used for series resummation to tackle convergence problems. The strategy consists of estimating a certain function using a quotient $B_{L/M}(x)$ of order $N = L + M$. For instance, given a asymptotic expansion $Z(x) = \sum_{n=0}^{\infty} z_n x^n$, where z_n and x are the expansion coefficients and the variable, respectively, the corresponding Padé approximant of order $[L/M]$ would be a ratio of two polynomials of order L on the numerator and

M on the denominator [33],

$$B_{L/M}(x) = \frac{\sum_{n=0}^{L} p_n x^n}{1 + \sum_{n=1}^{M} q_n x^n}. \tag{2.12}$$

The coefficients are normalized by assigning $q_0 = 1$ and determined by ensuring that the Padé approximant matches the Taylor series of $Z(x)$ through order $L + M$. Ergo,

$$Z(x) = B_{[L/M]}(x) + \mathrm{O}(x^{L+M+1}). \tag{2.13}$$

In practice, the coefficients of the Padé approximant are obtained by solving a system of $L + M + 1$ linear equations, which are obtained by setting the derivatives of the target function and its Padé approximant equal at $x = 0$. Specifically, from $\left.\frac{\mathrm{d}^n Z(x)}{\mathrm{d}x^n}\right|_{x=0} = \left.\frac{\mathrm{d}^n B_{L/M}(x)}{\mathrm{d}x^n}\right|_{x=0}$ one obtains [33]:

$$\begin{array}{lllll}
 & & & z_0 & = p_0 \\
 & & z_1 & +z_0 q_1 & = p_1 \\
 & z_2 & +z_1 q_1 & +z_0 q_2 & = p_2 \\
 & & & & \vdots \\
z_L & +z_{L-1} q_1 & +\cdots & +z_0 q_L & = p_L \\
z_{L+1} & +z_L q_1 & +\cdots & +z_{L-M+1} q_M & = 0 \\
 & & & & \vdots \\
z_{L+M-1} & +z_{L+M-2} q_1 & +\cdots & +z_{L-1} q_M & = 0 \\
z_{L+M} & +z_{L+M-1} q_1 & +\cdots & +z_L q_M & = 0
\end{array} \tag{2.14}$$

A table of Padé approximants can be easily tabulated by setting different values for L and M. Because it is a rational function, the singularities of a Padé approximant in the complex plane are poles. The Padé approximant, then, is less suitable for modelling functions with algebraic branch points or essential singularities.

2.1.3 Meijer-G function

A Meijer-G function is a very general expression that can represent most special functions by suitable choices for its parameters.[34, 35]. The set of integers m, n, p, and q determine the order of the Meijer-G function. Given a set of parameters $\{a_1, \cdots, a_p\}$ and $\{b_1, \cdots, b_q\}$, the Meijer-G function is expressed as a function of z and r,

$$G_{p,q}^{m,n}\left(\begin{matrix}a_1,\cdots,a_n;a_{n+1},\cdots,a_p\\ b_1,\cdots,b_m;b_{m+1},\cdots,b_q\end{matrix}\middle| x;\, r\right) = \frac{1}{2\pi i} \times \int_L \frac{\prod_{j=1}^{m}\Gamma(b_j+s)\prod_{j=1}^{n}\Gamma(1-a_j-s)}{\prod_{j=n+1}^{p}\Gamma(a_j+s)\prod_{j=m+1}^{q}\Gamma(1-b_j-s)} x^{-s/r}\,\mathrm{d}s, \tag{2.15}$$

Here, $0 \le m \le q$ and $0 \le n \le p$, and Γ is the gamma function:

$$\Gamma(x) = \int_0^\infty t^{x-1}e^{-t}\mathrm{d}t. \tag{2.16}$$

In most applications of the Meijer-G function, one chooses $r = 1$.

The Meijer-G function can mimic singularities beyond poles. Unfortunately, until recently, there was no simple way, analogous to Eq. (3.4) for the Padé

approximant, to determine the parameters in a Meijer-G approximant.

2.1.4 Borel approach

Recall that for any positive integer, the Gamma function can also be expressed as a factorial function:

$$\Gamma(x) = (x-1)! = \int_0^\infty t^{x-1} e^{-t} dt \tag{2.17}$$

The Borel method consists of using a factorial function to regularize divergent series.[36]. The basic idea is that if one observes a series where the size of the coefficients is diverging,

$$Z(x) = \sum_{n=0}^{\infty} z_n x^n \tag{2.18}$$

then it would be beneficial to divide the coefficients by $n!$.[37]. This defines the Borel transformation of $Z(x)$,

$$B_Z(t) = \sum_{n=0}^{\infty} b_n t^n \tag{2.19}$$

$$b_n = \frac{z_n}{n!} \tag{2.20}$$

To invert the Borel transformation, it is beneficial to rewrite (2.18) using the integral form of the Gamma function,

$$\begin{aligned} Z(x) &= \sum_{n=0}^{\infty} z_n x^n \frac{\Gamma(n+1)}{n!} \\ &= \int_0^{\infty} \left(\sum_{n=0}^{\infty} \frac{z_n}{n!} x^n \right) t^n e^{-t} dt \\ &= \int_0^{\infty} \left(\sum_{n=0}^{\infty} \frac{z_n}{n!} (xt)^n \right) e^{-t} dt \\ &= \int_0^{\infty} B_Z(xt) e^{-t} dt \end{aligned} \tag{2.21}$$

If the coefficients z_n grow factorially, the Borel transform removes such growth yielding a finite nonzero radius of convergence. In summary, for a given divergent expansion $Z(x) = \sum_{n=0}^{\infty} z_n x^n$, the Borel method follows these steps:

1. Borel transform the coefficients.

$$b_n = \frac{z_n}{n!} \tag{2.22}$$

2. Sum the Borel-transformed series in the Borel plane.

$$B_Z(t) = \sum_{n=0}^{\infty} b_n t^n \tag{2.23}$$

3. Use an integral related to the Laplace transform to return (an approxi-

mation to) the original function,

$$Z_B(x) = \int_0^\infty e^{-t} B(tx) \mathrm{d}t \tag{2.24}$$

In practice, one usually truncates the original Taylor expansion and therefore the Borel-transformed series in Eq. 2.19 is also truncated. Different resummations of the series in the Borel plane give different results when transformed back.

In the Borel-Padé method is similar, but the summation in the Borel plane is done using a Padé approximant.[38]. This requires solving the set of equations to find the parameters p_n and q_n that give the best fit. This method is summarized in the following steps:

1. Borel transform the coefficients.

$$b_n = \frac{z_n}{n!} \tag{2.25}$$

2. Summation in the Borel plane using a Padé approximant.

$$B_{L/M}(t) = \frac{\sum_{n=0}^{L} p_n t^n}{1 + \sum_{n=1}^{M} q_n t^n}. \tag{2.26}$$

3. Take the Laplace transform to return the Borel sum.

$$Z_B(x) = \int_0^\infty e^{-t} B_{L/M}(tx) \mathrm{d}t \tag{2.27}$$

The Borel-Padé approach is attractive because the integral in Eq. 2.27 can be evaluated exactly using exponential integrals.

Borel-Padé approximants converge slowly when the Borel-transformed series has a branch cut. However, generalized hypergeometric functions have a built-in branch cut singularity, and potentially can model the series 2.19 more accurately.[38, 25, 26].

Mera *et al.* present an algorithm that improves the Borel-Padé resummation using Meijer-G functions.[25, 26]. One of the differences is that the coefficients of the series must be normalized, $z_0 = 1$, and the first $N+1$ terms of the series must be known, where N is the order of the approximant. After the Borel transform $b_n = \frac{z_n}{n!}$, the ratios of the new consecutive coefficients are obtained. Then, a generalized hypergeometric ansatz is made for each of the ratios by setting it equal to a Padé approximant function of m, the index of the ratio. The order of the Padé, both L and M, is fixed to be integer $l = (N-1)/2$. Note that in the case of even orders, l is a fraction, so the first term of the series can be subtracted, and the remaining terms are normalized so that $z_0 = 1$. The one-subtracted expansion can then be treated with odd order $N-1$ resummation, and the removed term can be added to the Meijer-G function in the end.

The basic algorithm for extracting the Meijer-G approximant of N^{th} order, where N is odd, is as follows:

1. Normalize the function so that $z_0 = 1$. When N is odd,

$$\tilde{Z}(x) = \frac{Z(x)}{z_0} \approx \sum_{n=0}^{N} \frac{z_n}{z_0} x^n \tag{2.28}$$

$$= \sum_{n=0}^{N} \tilde{z}_n x^n \tag{2.29}$$

$$\tilde{z_n} = \frac{z_n}{z_0} \tag{2.30}$$

When N is even we use the one-subtracted series,

$$\tilde{Z}(x) = \frac{Z(x) - z_0}{z_1 x} \approx \sum_{n=0}^{N-1} \frac{z_{n+1}}{z_1} x^n \tag{2.31}$$

$$= \sum_{n=0}^{N-1} \tilde{z}_n x^n \tag{2.32}$$

$$\tilde{z_n} = \frac{z_{n+1}}{z_1} \tag{2.33}$$

In both cases there are an even number of terms in the summation, and $\tilde{z_0} = 1$.

2. Borel transform $\tilde{Z}(x)$.

$$B_{\tilde{Z}}(t) = \sum_{n=0}^{\infty} \frac{\tilde{z}_n}{n!} t^n = \sum_{n=0}^{\infty} b_n t^n \tag{2.34}$$

$$\approx \sum_{n=0}^{N} b_n t^n \tag{2.35}$$

$$b_n = \frac{\tilde{z}_n}{n!} \tag{2.36}$$

3. Calculate ratios of consecutive terms in the Borel series. For $0 \leq m \leq$

$N-1$.

$$r(m) = \frac{b_{m+1}}{b_m} \tag{2.37}$$

4. Fit the ratios, $r(m)$ with a Padé approximant, $B_{\left[\frac{N}{2}/\frac{N}{2}\right]}$. This gives a system of N equations, $0 < m < N-1$,

$$r(m) = \frac{b_{m+1}}{b_m} = \frac{\sum_{n=0}^{\frac{N}{2}} p_n m^n}{1 + \sum_{n=1}^{\frac{N}{2}} q_n m^n} \tag{2.38}$$

5. This can be rearranged into a linear system of equations, which are then solved for the $\{p_n\}$ and $\{q_n\}$.

6. To fit the Borel-transformed function, $B_{\tilde{Z}(t)}$, we find the roots of the numerator and the denominator of our approximation to $r(m)$,

$$\sum_{n=0}^{l} p_n x^n = 0 \tag{2.39}$$

$$1 + \sum_{n=1}^{l} q_n y^n = 0 \tag{2.40}$$

Label the roots $\vec{x} = \left[x_1, x_2, \ldots, x_{\frac{N}{2}}\right]$ and $\vec{y} = \left[y_1, y_2, \ldots, y_{\frac{N}{2}}\right]$.

7. Determine the generalized hypergeometric approximant ${}_{l+1}F_l$ in the Borel plane, where $l = \frac{N}{2}$

$$B_{\tilde{Z}}(t) =_{l+1} F_l\left(\vec{x}, \vec{y}, \frac{p_l}{q_l} t\right) \tag{2.41}$$

8. Take the Laplace transform of the hypergeometric function to return the

Borel resummation,

$$\tilde{Z}(x) \approx \int_0^\infty e^{-t} B_{\tilde{Z}}(tx) \mathrm{d}t \tag{2.42}$$

$$\tilde{Z}(x) \approx \frac{\prod_{i=1}^{l} \Gamma(-y_i)}{\prod_{i=1}^{l}(-x_i)} G^{l+2,1}_{l+1,l+2}\left(\begin{matrix} 1, -y_1, \cdots, -y_l \\ 1, 1, -x_1, \cdots, -x_l \end{matrix} \middle| -\frac{q_l}{p_l x} \right). \tag{2.43}$$

2.2 Density Functional Theory

In density-functional theory (DFT), the 3-variable ground-state electron density $n(x, y, z)$ replaces the $3N$-variable wavefunction,
$\Psi\left(x_1, y_1, z_1; x_2, y_2, z_2; \ldots; x_N, y_N, z_N\right)$ as the fundamental descriptor of an N-electron molecule. On its surface, this dramatically reduces the complexity of quantum-mechanics, because the N-electron Schrödinger equation is replaced by an equation using density functionals. Ideally, a DFT-based method scales linearly as O(N), but limitations arise because the universal Hohenberg-Kohn functional is not known in any exact, explicit, form.

The most common approximation is the Kohn-Sham DFT (KSDFT), which introduces orbitals as auxiliary quantities with which to compute the noninteracting kinetic energy. Determining the orbitals requires solving a system of coupled one-electron equations (the Kohn-Sham equations), which means that one must (either implicitly or explicitly) diagonalize a one-electron Hamiltonian, with inherent cost $O(N^3)$ (which may nonetheless be reduced for large systems). If the noninteracting kinetic energy were expressed as an explicit

density functional, however, near-ideal scaling can be recovered, as the cost of evaluating the kinetic energy then grows linearly, in proportion to the volume of the system.

Many different approaches have been taken to the kinetic energy density functional [10], but this study focuses on the gradient expansion approximation. Nonetheless, a gradient expansion of the kinetic energy is not accurate enough for atoms and molecules, mainly because higher-order terms diverge. This is not that surprising given the highly inhomogeneous nature of the electron density in molecular systems. This inhomogeneity can be mitigated with local pseudopotentials, at the cost of introducing still another approximation, which is of dubious accuracy in many cases. Resummation of the gradient expansion series by Padé approximants showed some improvement in accuracy.[23]. In this work, Padé approximants and hypergeometric resummations are studied and compared to the truncated sum of the series.

2.2.1 Thomas-Fermi model

In 1927, Thomas and Fermi presented the first attempt to model electronic structure using only the electron density [14, 15, 39]. Their model estimates the electronic distribution by dividing molecular space into small cubes, each of which contained a uniform gas of noninteracting electrons. In this approximatio, the kinetic energy of these volume elements can be determined exactly, and was then integrated to approximate the total noninteracting kinetic energy

of the system, giving the Thomas-Fermi functional,

$$T_{TF}[n] = C_{TF} \int n^{5/3} d\mathbf{r} = \frac{3}{10}(3\pi^2)^{2/3} \int n^{5/3} d\mathbf{r} \tag{2.44}$$

This functional is sometimes called the local density approximation (LDA). As its name and expression implies, the estimation of the local kinetic energy at the point $\mathbf{r}$ is based on the electron density at $\mathbf{r}$ only. In the original Thomas-Fermi model, exchange and correlation effects are neglected and the energy is given as an explicit functional of the electron density by the expression:

$$\begin{aligned} E_{TF}[n(\mathbf{r})] = C_{TF} \int n^{5/3} d\mathbf{r} + \sum_{A}^{\text{nuclei}} \int \frac{Z_A}{|\mathbf{r} - \mathbf{R}_A|} n(\mathbf{r})\, \mathrm{d}\mathbf{r} \\ + \frac{1}{2} \int \int \frac{n(\mathbf{r}_1) n(\mathbf{r}_2)}{|\mathbf{r}_1 - \mathbf{r}_2|}\, \mathrm{d}\mathbf{r}_1\, \mathrm{d}\mathbf{r}_2, \end{aligned} \tag{2.45}$$

Here Z_A and $\mathbf{R}_A$ denote the atomic number and positions of the atomic nuclei. The calculation of E_{TF} is fast, but it is only exact for the homogeneous gas of non-interacting electrons. The strategy of determining E_{TF} by minimizing the energy expression with respect to the density was assumed to be valid in the original work Thomas and Fermi and subsequent studies, all the way until 1964.

2.2.2 Hohenberg and Kohn Theorems

Two key precepts of wavefunction-based quantum mechanics are that

1. Any observable property of an system can be determined from its wave-

function.

2. The ground-state wavefunction of a system can be determined by minimizing the energy, $\left\langle \Psi \left| \hat{H} \right| \Psi \right\rangle$ over the space of physically permissible (e.g., antisymmetric, normalized) wavefunctions.

Analogous theorems for the ground-state electron density were established by Hohenberg and Kohn in their 1964 paper. The first theorem states that: " *The external potential* $\nu(\mathbf{r})$ *is (to within a constant) a unique functional of the ground-state electron density,* $n(\mathbf{r})$. Since $\nu(\mathbf{r})$ determines $\hat{H}$, which is sufficiently to determine the wavefunctions (by solving the Schrödinger equation), we see that all observable properties of a system can be expressed as functionals of $n(\mathbf{r})$." In particular, there is an *exact* density functional for the ground-state energy of a system, and all the components thereof. The proof of the theorem by *reductio ad absurdum* is straightforward and is shown in Ref. [40]. Symbolically, the first Hohenberg-Kohn theorem can be summarized by

$$n_0(\mathbf{r}) \longrightarrow \{N, \nu(\mathbf{r})\} \longrightarrow \hat{H} \longrightarrow \Psi_0 \longrightarrow E_0, \ldots$$

The second Hohenberg-Kohn theorem indicates that the ground-state electron density, $n_0(\mathbf{r})$, yields the lowest energy; all other trial densities would give a higher energy that E_0.

Rather than write the ground-state energy directly as a functional of $n(\mathbf{r})$, it is convenient to write it as a sum of density functional contributing density functionals,

$$E[n(\mathbf{r})] = T[n(\mathbf{r})] + V_{ee}[n(\mathbf{r})] + V_{ne}[n(\mathbf{r})], \tag{2.46}$$

where T is the kinetic energy, V_{ee} is the sum of all the electron-electron interactions, and V_{ne} is the external potential energy due to nucleus-electron interactions. The latter is easily expressed as an explicit density functional,

$$V_{ne}[n(\mathbf{r})] = \sum_{A}^{\text{nuclei}} \int \frac{Z_A}{|\mathbf{r} - \mathbf{R}_A|} n(\mathbf{r})\, \mathrm{d}\mathbf{r} \tag{2.47}$$

The first two terms must be approximated, and are often combined into the universal Hohenberg-Kohn functional F. $F[n]$ is universal in the sense that its mathematical form does not depend explicitly on $\{N, Z_A, \mathbf{R}_A\}$ variables; therefore the same F can be used for *any* system.

$$F[n(\mathbf{r})] = T[n(\mathbf{r})] + V_{ee}[n(\mathbf{r})] \tag{2.48}$$

This approach, which is often called Hohenberg-Kohn DFT (HKDFT) is exact, follows the variational principle, and scales linearly, but unfortunately, the exact mathematical expression for F is not known. The classical electron-electron repulsion that contributes to V_{ee} can also be written as an explicit and exact density functional. Specifically, the classical Coulomb repulsion is given by:

$$J[n(\mathbf{r})] = \frac{1}{2} \int \int \frac{n(\mathbf{r}_1) n(\mathbf{r}_2)}{|\mathbf{r}_1 - \mathbf{r}_2|}\, \mathrm{d}\mathbf{r}_1\, \mathrm{d}\mathbf{r}_2. \tag{2.49}$$

The remaining contribution includes exchange and correlation effects. Explicit exact functionals for these contributions, together with the kinetic energy functional are still unknown. Because of this, HKDFT cannot be used for practical electron structure calculations without further approximations. However, as soon as approximations are made, the variational principle is not guaranteed (it is possible to obtain results below the true energy). However, because HKDFT is computationally inexpensive and amenable to linear-scaling techniques, it is very attractive. Approximations like as the Thomas-Fermi model retain the appealing low computational cost of HKDFT, but accuracy is severely compromised, even when an exchange correction is included.

The Thomas-Fermi-Dirac (TFD) model extends the Thomas-Fermi model to include exchange. Like Thomas and Fermi, Dirac used a periodic system with electrons in a cubic unit cell to describe a noninteracting homogeneous gas of electrons [41]. The kinetic energy is given by T_{TF}, but the exchange energy is no longer ignored, but computed exactly from the Hartree-Fock exchange-energy expression,

$$K_D[n] = C_X \int n^{4/3} d\mathbf{r} = \frac{3}{4}(3\pi)^{1/3} \int n^{4/3} d\mathbf{r}. \tag{2.50}$$

The TFD model is a good first approximation, but its accuracy is not acceptable [42]. One can systematically improve the functionals for kinetic energy and exchange via a gradient expansion. That is, one can relax the assumption that there is a noninteracting homogeneous gas by adding corrections for inhomogeneity. However, before we assess this strategy, it is important to

first discuss how the *exact* values for the kinetic and exchange energy can be computed.

2.2.3 Kohn-Sham DFT

Hohenberg and Kohn showed that the energy can be obtained as a functional of the density. The only problem is that no exact explicit mathematical expression of the functional is known, so the Hohenberg-Kohn theorems merely prove the existence of a computational methodology based on the ground-state electron density; they give no hint as to how to transform this methodology into a practical computational method for studying chemical systems. A year after Hohenberg and Kohn's paper, Kohn and Sham proposed a strategy that turned DFT into a practical tool for electronic calculations. Perhaps inspired by the work of Thomas, Fermi, and Dirac for uniform electron gasses of non-interacting electrons, they introduced a reference state consisting of noninteracting electrons, but with the same (nonuniform!) density as the true physical system with interacting electrons. The kinetic energy of the reference system can be calculated using orbitals,

$$T_s[\{\psi_i\}] = -\frac{1}{2}\sum_{i\in\text{occ}} \left\langle \psi_i \left| \nabla^2 \right| \psi_i \right\rangle, \tag{2.51}$$

As in HKDFT, in KSDFT the classical Coulomb energy J is also used to recover the classical electrostatic self-repulsion of the electron density. The remaining errors are assigned to the exchange-correlation term E_{xc}. The ground-

state electronic energy is thus expressed as

$$E[n(\mathbf{r})] = T_s[n(\mathbf{r})] + V_{ne}[n(\mathbf{r})] + J[n(\mathbf{r})] + E_{xc}[n(\mathbf{r})], \tag{2.52}$$

The exchange-correlation energy includes the residual part of the kinetic energy (due to electron correlation), and the non-classical electrostatic contributions (including corrections due to the Pauli principle and electron correlation). The exchange-correlation energy explicitly removes the self-interaction of electrons. E_{xc} is typically written as an integral of the exchange and correlation density ε_{xc} over all space,

$$E_{xc}[n(\mathbf{r})] = \int \varepsilon_{xc}(n, \nabla n, \nabla^2 n, \cdots) d\mathbf{r} \tag{2.53}$$

The local density approximation (LDA) is the lowest rung of approximations forE_{xc}, where $\varepsilon_{xc}(\mathbf{r})$ only depends on electron density itself, at the same point in space, $n(\mathbf{r})$. The most intuitive approach for improving $\varepsilon_{xc}(\mathbf{r})$ is to include information about the electron density at points near $\mathbf{r}$ by using derivatives of the electron density. The second rung of approximations includes the first derivative; functionals of this form are called generalized gradient approximations (GGAs). Going beyond GGAS, on the third rung of the density-functional hierarchy one includes information about higher-order derivatives and/or the kinetic energy density (e.g., from the integrand in Eq. 2.50; these are called meta-GGAs). One can also include truly nonlocal information; at the fourth rung of the hierarchy one includes other information from the oc-

cupied Kohn-Sham orbitals, most frequently the exact exchange energy (from the Hartree-Fock energy expression) or the exchange-energy density. These functionals, especially the ones that use the Hartree-Fock exchange expression, are commonly called hybrid density functionals. Hybrid functionals and meta-GGAs generally require information about the Kohn-Sham orbitals, and are thus inapplicable in HKDFT.

Like HKDFT, KSDFT is exact in principle. However, once an explicit and approximate functional is chosen to approximate E_{xc}, the variational principle is generally no longer valid. Therefore, it is difficult to validate the quality of the functional. It is especially complicated because improving approximations by moving from LDA to GGA to meta-GGA to hybrid-GGA approaches does not guarantee better accuracy. I.e., when choosing a suitable functional, one must consider the the characteristics of the system of interest: different (types of) functionals work better for different (types of) chemical systems.

2.2.4 Kinetic Energy Density Functionals

When approximating the kinetic energy functional, one encounters difficulties analogous to those encountered in the exchange-correlation energy functional. However, the kinetic energy makes a much larger contribution to the exact energy and, as noted by Ruedenberg and Kutzelnigg, makes a decisive contribution to chemical binding phenomena. Relative to the exchange-correlation functional, the kinetic energy functional must be more accurate.

Many techniques for approximating the noninteracting kinetic energy density have been proposed. Some of these techniques are less suited to HKDFT because they make it difficult to achieve linear scaling with HKDFT. However, by analogy to the exchange-correlation energy functional, it is permissible to approximated the noninteracting kinetic energy density functional (KEDF), $T_s[n]$ as an integral of the kinetic energy density over all space,

$$T_s[n(\mathbf{r})] = \int t(n, \nabla n, \nabla^2 n, \cdots) d\mathbf{r} \tag{2.54}$$

The kinetic energy density for the Thomas-Fermi model is exact for a homogeneous noninteracting gas of electrons and is given by the integrand:

$$t_0 = t_{TF} = C_{TF} n^{5/3} \tag{2.55}$$

The most straightforward approach for including inhomogeneity in the kinetic energy density is by including dependence on higher-order derivatives of the density, in analogy to GGA (and kinetic-energy-density-free meta-GGA) functionals for the exchange-correlation energy. The von Weizsäcker KEDF was the first correction that includes the gradient of the density,

$$t_W = \frac{1}{8} \frac{|\nabla n|^2}{n} \tag{2.56}$$

The von Weizsäcker functional is exact for systems with nondegenerate ground states and up to two electrons; it is a strict lower bound to the true KEDF.

However, when combined with Thomas-Fermi theory, the Weizsäcker correction is too large, and only a fraction of t_W is necessary.

A more general form of the gradient expansion approximation of the KEDF is

$$T_s[n] = T_0 + T_2 + T_4 + \dots \tag{2.57}$$

$$= \sum_{k=0}^{\infty} \int t_{2k}[n(\mathbf{r}), \nabla n(\mathbf{r}), ..., \nabla^{2k} n(\mathbf{r})] d\mathbf{r} \tag{2.58}$$

Notice that odd order terms are not included because they are zerol The zeroth-order term is the Thomas-Fermi KEDF. Kirzhnits [17] derived the second-order term, which turns out to be $\frac{1}{9}^{\text{th}}$ of the Weizsäcker KEDF,

$$t_2 = \frac{1}{72} \frac{|\nabla n|^2}{n} \tag{2.59}$$

Following the same methodology as Kirzhnits, Hodges [18] derived the fourth-order term:

$$t_4 = \frac{(3\pi^2)^{-2/3}}{540} n^{1/3} \left(\left(\frac{\nabla^2 n}{n} \right)^2 - \frac{9}{8} \frac{|\nabla n|^2 \nabla^2 n}{n^3} + \frac{1}{3} \frac{|\nabla n|^4}{n^4} \right). \tag{2.60}$$

Similarly, Murphy [19] obtained the sixth order term:

$$t_6 = \frac{(3\pi^2)^{-4/3}}{45360} n^{-1/3} \left[13 \frac{\left|\nabla \left(\nabla^2 n\right)\right|^2}{n^2} + \frac{2575}{144} \left(\frac{\nabla^2 n}{n}\right)^3 \right.$$
$$+ \frac{249}{16} \frac{|\nabla n|^2}{n^2} \frac{\nabla^4 n}{n} + \frac{1499}{18} \frac{|\nabla n|^2}{n^2} \left(\frac{\nabla^2 n}{n}\right)^2$$
$$- \frac{1307}{36} \frac{|\nabla n|^2}{n^2} \frac{\nabla n \cdot \nabla \left(\nabla^2 n\right)}{n^2} + \frac{343}{18} \left(\frac{\nabla n \cdot \nabla \nabla n}{n^2}\right)^2$$
$$\left. + \frac{8341}{72} \frac{\nabla^2 n}{n} \frac{|\nabla n|^4}{n^4} - \frac{1600495}{2592} \frac{|\nabla n|^6}{n^6} \right]. \tag{2.61}$$

The second and fourth order terms are actually more complicated. They result from the partial integration of the asymptotic gradient expansion described by Jennings [20]. The complete second order term is given by:

$$t_2^J = \frac{1}{72} \frac{|\nabla n|^2}{n} + \frac{1}{6} \nabla^2 n, \tag{2.62}$$

The second term integrates to zero for any system with rapidly decaying electron density, including atoms and molecules, and so this term is usually discarded. However, the additional term does contribute to the kinetic-energy density. Similarly, the complete fourth-order term is:

$$t_4^J = \frac{(3\pi^2)^{-2/3}}{4320} n^{1/3} \left(12 \frac{\nabla^4 n}{n} - 30 \frac{\nabla n \cdot \nabla (\nabla^2 n)}{n^2} \right.$$
$$- 14 \left(\frac{\nabla^2 n}{n}\right)^2 - 7 \frac{\nabla^2 (|\nabla n|^2)}{n^2}$$
$$\left. + \frac{140}{3} \frac{|\nabla n|^2 \nabla^2 n}{n^3} + \frac{92}{3} \frac{\nabla n \cdot \nabla \left(|\nabla n|^2\right)}{n^3} - 48 \frac{|\nabla n|^4}{n^4} \right). \tag{2.63}$$

Both the truncated and complete forms of the gradient expansion will be considered here. The complete terms give different answers because we resum the series expansions for the kinetic energy density first, then integrate r. Since the additional terms can carry information that is useful for predicting the kinetic energy density, they should be considered. Sim *et al.* [2] also stress on the importance of analyzing the kinetic energy density when testing a functional.

Chapter 3

Methodology

3.1 Computational Details

The calculations of the kinetic energy approximations were made using `HORTON`[1], specifically the *iodata*, *grid* and *gbasis* packages. The initial molecular data, mainly the density matrix, is loaded with *iodata* from a Gaussian 16 [43] calculation at either UHF/UGBS or UPBEPBE/UGBS level of theory. The energy partition option in Gaussian 16 is utilized to find the reference Kohn-Sham kinetic energy. Note that while UPBEPBE exchange-correlation functional is not exact, the kinetic energy from a UPBEPBE Kohn-Sham calculation exactly corresponds to the electron density from a UPBEPBE calculation in the basis-set limit. By using a the large, uncontracted, UGBS basis set, we ensure that the reference kinetic energy is very close to the true value (it will always be slightly too high) associated with the UPBEPBE calculation.

While the Hartree-Fock kinetic energy and the Kohn-Sham kinetic energy are different, they are very close, and it is common in the literature to study kinetic energy functionals for the Hartree-Fock kinetic energy, even though this does not strictly fit into the KSDFT framework. We use the UHF/UGBS results so that we can compare to these results from the literature.

A total of 21 functionals for the kinetic-energy functional are tested; six of these functionals include a parameterization step using all other molecules in the test set. When we include the complete form of the terms of the gradient expansion (i.e., including the terms that integrate to zero over all space) we use the index j. The test set comprises the atoms H-Ar and some small molecules (H_2, HF, LiH, LiF, N_2, H_2O, NH_3, and CH_4).

3.2 Methodology

Consider the gradient expansion of the kinetic energy density,

$$t(\mathbf{r}) = t_0(\mathbf{r}) + t_2(\mathbf{r}) + t_4(\mathbf{r}) + \cdots . \tag{3.1}$$

The accuracy from gradient corrections is limited because this series does not converge. Not only do the higher-order terms become larger and larger, individual terms diverge in certain regions (e.g., near the electron-nuclear cusp in the electron density). In general, it is observed that t_2 improves the approximation, but t_4 does not always help. The following figure of the radial distribution of the kinetic energy density summed up to different orders shows

that t_4 adds a singularity near the nucleus and deviates from the exact kinetic energy density at long distances.

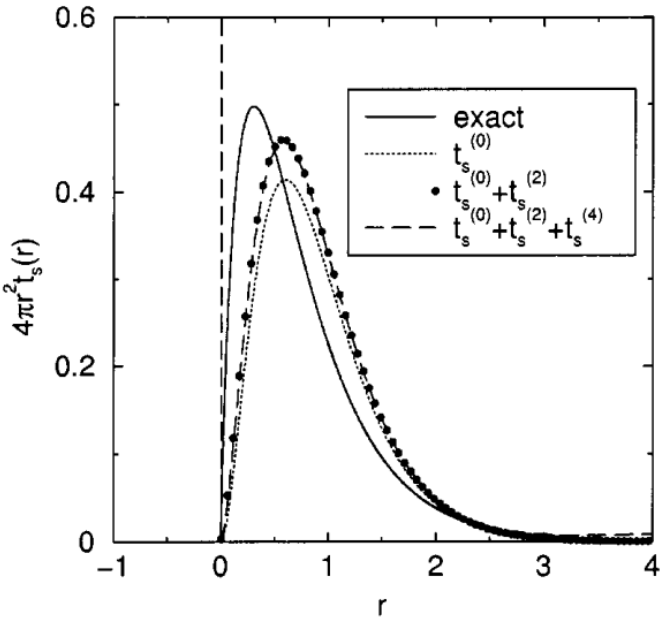

Figure 3.1: Gradient expansion approximated and exact t_s kinetic energy densities for the hydrogen atom. Figure taken from Ref. [2].

Clearly, the gradient expansion of the kinetic energy density is a non-convergent series, and the truncation of the summation can lead to an asymptotic series with partial information about the original functional [23, 21].

Fig. 3.2 shows that the radial distributions of t_4 and t_6 term diverge far from the nucleus and near the nucleus. This is the general behaviour for all atoms that were studied. The divergence of t_4 is not as pronounced as t_6 as the slope and values of the fourth-order correction is smaller. As expected, truncation up to t_2 is usually the best approximation for the kinetic energy.

In this study, several functionals based on Padé and Meijer-G approximants

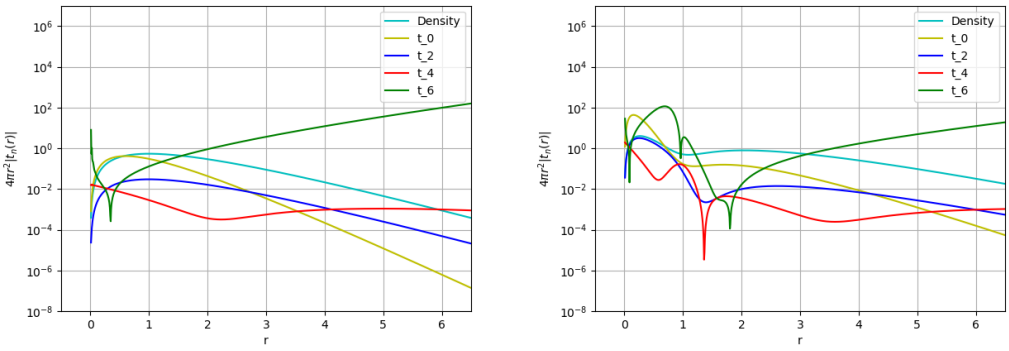

(a) H

(b) Be

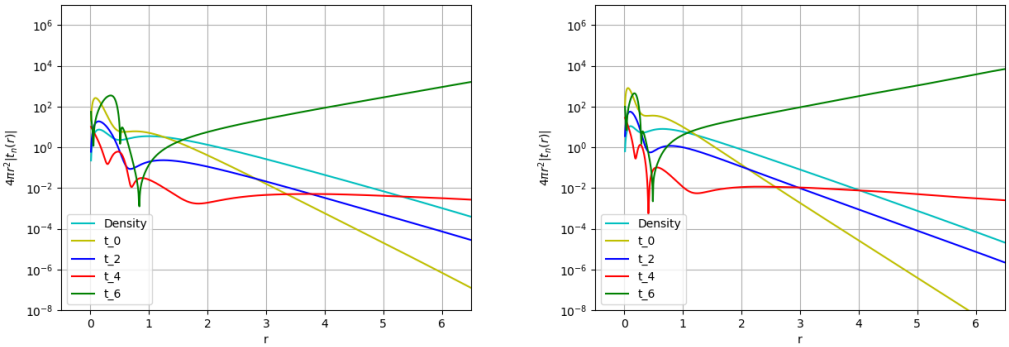

(c) N

(d) Ne

Figure 3.2: Plots of the radial distribution of the density and the terms of the gradient expansion of the kinetic energy density for different atoms on a logarithmic scale. The coefficients are obtained with Gaussian 16 UHF/UGBS and the gradient expansion is calculated using HORTON 3.

were used to resum the divergent expansion of the kinetic energy. The Padé approximant is useful for recovering information about the higher order terms when they are small and avoiding them when they are large [23]. Low-order Meijer-G approximants often perform better than Padé approximants because they intrinsically include a branch cut, while the Padé only models poles [26]. For reference, we compare to the thoroughly studied gradient expansion ap-

proximation functionals T_0, T_0+T_2, $T_0+T_2+T_4$, and $T_0+T_2+T_4+T_6$, which are calculated by integration over molecular space [**?**, 21].

Following the Meijer-G approximant method, the series is normalized by dividing by the first term,

$$\frac{t(\mathbf{r})}{t_0(\mathbf{r})} = 1 + \frac{t_2(\mathbf{r})}{t_0(\mathbf{r})} + \frac{t_4(\mathbf{r})}{t_0(\mathbf{r})} + \cdots . \tag{3.2}$$

A perturbation parameter x, which gives back the original gradient expansion when $x = 1$, is then introduced,

$$\frac{t(\mathbf{r})}{t_0(\mathbf{r})} = 1 + z_1(\mathbf{r})x + z_2(\mathbf{r})x^2 + \cdots , \tag{3.3}$$

where $z_1 = \frac{t_2(\mathbf{r})}{t_0(\mathbf{r})}$, $z_2 = \frac{t_4(\mathbf{r})}{t_0(\mathbf{r})}$, and so on.

3.2.1 Padé Resummation

The simplest method consists of using a Padé approximant to resum the kinetic energy $t(\mathbf{r})$. The derivation of the lowest order approximant $B_{0/1}(x)$ is straightforward. Taking the set of equations 3.4, we obtain the following:

$$\begin{aligned} 1 &= p_0 \\ \frac{t_2(\mathbf{r})}{t_0(\mathbf{r})} + q_1 &= p_1 = 0 \end{aligned} \tag{3.4}$$

Note that $p_1 = 0$ because $L = 0$. Solving for the parameters, and inserting

them into the expression for the Padé approximant, gives the following:

$$B_{0/1}(x) = \frac{1}{1 - \frac{t_2(\mathbf{r})}{t_0(\mathbf{r})}x} = \frac{t_0(\mathbf{r})}{t_0(\mathbf{r}) - t_2(\mathbf{r})} \tag{3.5}$$

In the final step, it is already taken into account that $x = 1$. The kinetic energy is then expressed as

$$t(\mathbf{r}) = t_0(\mathbf{r})B_{0/1}(x) = \frac{t_0^2(\mathbf{r})}{t_0(\mathbf{r}) - t_2(\mathbf{r})}. \tag{3.6}$$

Clearly, singularities arise when $t_0(\mathbf{r}) = t_2(\mathbf{r})$. A possible solution is to use a different function when this is the case, such as:

$$t(\mathbf{r}) = \begin{cases} t_0(\mathbf{r}) & \left|\frac{t_0(\mathbf{r}) - t_2(\mathbf{r})}{t_0(\mathbf{r})}\right| \ll 1 \\ \frac{t_0^2(\mathbf{r})}{t_0(\mathbf{r}) - t_2(\mathbf{r})} & \text{otherwise} \end{cases} \tag{3.7}$$

Two approximations were proposed to ensure this behaviour with a smooth transition. The first suggestion uses the softplus activation function, also called the smooth ReLU (rectified linear unit) function.

$$\text{softReLU}_\xi(x) = \ln(1 + e^{x\xi}) \tag{3.8}$$

Notice that the function is not zero at the origin and at big values of x, the function returns the argument of the exponential. With the following

expression, the transition from one case to the other can be softened,

$$t_\xi(\mathbf{r}) = t_0(\mathbf{r}) \left(\frac{1}{a + \text{softReLU}_\xi\left(-\frac{t_2(\mathbf{r})}{t_0(\mathbf{r})}\right)} \right). \tag{3.9}$$

The parameter ξ can be fitted to a certain data set and to get a, certain consideration must be made. When $t_2(\mathbf{r}) = 0$, one would also expect to recover $t_\xi(\mathbf{r}) = t_0(\mathbf{r})$. Taking this into account and substituting in the previous equation,

$$\begin{aligned} 1 &= a + \text{softReLU}_\xi(0) \\ 1 &= a + \frac{1}{\xi}\ln(1+1) \\ a &= 1 - \frac{\ln(2)}{\xi} \end{aligned} \tag{3.10}$$

This function also shows reasonable behaviour when $t_2(\mathbf{r}) \longrightarrow \pm\infty$. For the positive case, $t_\xi(\mathbf{r})$ approaches $\frac{t_0(\mathbf{r})}{a}$ and for the negative case, $t_\xi(\mathbf{r}) \longrightarrow 0$. Also, note that when the argument of the softReLU function is relatively big, then the expression becomes

$$t_\xi(\mathbf{r}) = t_0(\mathbf{r}) \left(\frac{1}{a - \xi\left(-\frac{t_2(\mathbf{r})}{t_0(\mathbf{r})}\right)} \right). \tag{3.11}$$

The other regularizing function proposed is based on a hyperbolic tangent function that defines the contribution percentage of each case to give a gradual

transformation from one to the other.

$$t_\xi(\mathbf{r}) = t_0(\mathbf{r}) \left|\tanh\left(\frac{\xi t_0(\mathbf{r})}{t_0(\mathbf{r}) - t_2(\mathbf{r})}\right)\right| + \frac{t_0^2(\mathbf{r})}{t_0(\mathbf{r}) - t_2(\mathbf{r})}\left(1 - \left|\tanh\left(\frac{\xi t_0(\mathbf{r})}{t_0(\mathbf{r}) - t_2(\mathbf{r})}\right)\right|\right) \tag{3.12}$$

Here, the factor ξ must also be parameterized using a set of molecules or atoms, for which, the kinetic energy is already known. Other similar parameterized functionals were tested, including:

$$t_{\xi,B_{0/1,c}}(\mathbf{r}) = \xi\, t_0(\mathbf{r}) \tanh\left(\frac{\xi t_0(\mathbf{r})}{t_0(\mathbf{r}) - t_2(\mathbf{r})}\right) \tag{3.13}$$

$$t_{\xi,B_{0/1,d}}(\mathbf{r}) = \frac{t_0(\mathbf{r})}{\xi} \tanh\left(\frac{\xi t_0(\mathbf{r})}{t_0(\mathbf{r}) - t_2(\mathbf{r})}\right) \tag{3.14}$$

$$t_{\xi,B_{0/1,e}}(\mathbf{r}) = \frac{t_0(\mathbf{r})}{1 - \frac{1}{\xi}\tanh\left(\frac{\xi t_2(\mathbf{r})}{t_0(\mathbf{r})}\right)} \tag{3.15}$$

$$t_{\xi,B_{0/1,f}}(\mathbf{r}) = \frac{t_0(\mathbf{r})}{1 + \frac{\ln 2}{\xi} - \mathrm{softReLU}_\xi\left(\frac{t_2(\mathbf{r})}{t_0(\mathbf{r})}\right)} \tag{3.16}$$

The next order Padé approximant $B_{1/1}(x)$ can be obtained in the same manner. Solving the set of equations gives $p_0 = 1$, $p_1 = \frac{t_2^2(\mathbf{r}) - t_0(\mathbf{r})t_4(\mathbf{r})}{t_0(\mathbf{r})t_2(\mathbf{r})}$, and $q_1 = -\frac{t_4(\mathbf{r})}{t_2(\mathbf{r})}$. The final expression for the approximant is

$$t(\mathbf{r}) = t_0(\mathbf{r})B_{1/1}(x) = t_0(\mathbf{r}) + \frac{t_2^2(\mathbf{r})}{t_2(\mathbf{r}) - t_4(\mathbf{r})}. \tag{3.17}$$

When t_4 is a large number, the quotient form removes the contribution of such cases. On the other hand, when t_4 is small, it is taken into consideration in

the calculation.

The highest order Padé approximant that will be tested is $B_{2/1}(x)$ given by

$$t(\mathbf{r}) = t_0(\mathbf{r})B_{2/1}(x) = t_0(\mathbf{r}) + t_2(\mathbf{r}) + \frac{t_4^2(\mathbf{r})}{t_4(\mathbf{r}) - t_6(\mathbf{r})}. \tag{3.18}$$

Similar to the lowest order Padé approximant, a parameterized functional is proposed for $B_{1/1}$ and $B_{2/1}$ to avoid the singularities from the term with the quotient. They are given by the following expressions:

$$t_{\xi,B_{1/1,a}}(\mathbf{r}) = t_0(\mathbf{r}) + \frac{t_2(\mathbf{r})}{\xi}\tanh\left(\frac{\xi t_2(\mathbf{r})}{t_2(\mathbf{r}) - t_4(\mathbf{r})}\right) \tag{3.19}$$

$$t_{\xi,B_{1/1,b}}(\mathbf{r}) = t_0(\mathbf{r}) + \frac{t_2(\mathbf{r})}{1 - \frac{1}{\xi}\tanh\left(\frac{\xi t_4(\mathbf{r})}{t_2(\mathbf{r})}\right)} \tag{3.20}$$

$$t_{\xi,B_{1/1,c}}(\mathbf{r}) = t_0(\mathbf{r}) + \frac{t_2(\mathbf{r})}{1 - \frac{\ln 2}{\xi} + \mathrm{softReLU}_\xi\left(-\frac{t_4(\mathbf{r})}{t_2(\mathbf{r})}\right)} \tag{3.21}$$

$$t_{\xi,B_{1/1,d}}(\mathbf{r}) = t_0(\mathbf{r}) + \frac{t_2(\mathbf{r})}{1 + \frac{\ln 2}{\xi} - \mathrm{softReLU}_\xi\left(\frac{t_4(\mathbf{r})}{t_2(\mathbf{r})}\right)} \tag{3.22}$$

$$t_{\xi,B_{2/1,a}}(\mathbf{r}) = t_0(\mathbf{r}) + t_2(\mathbf{r}) + \frac{t_4(\mathbf{r})}{\xi}\tanh\left(\frac{\xi t_4(\mathbf{r})}{t_4(\mathbf{r}) - t_6(\mathbf{r})}\right) \tag{3.23}$$

$$t_{\xi,B_{2/1,b}}(\mathbf{r}) = t_0(\mathbf{r}) + t_2(\mathbf{r}) + \frac{t_4(\mathbf{r})}{1 - \frac{1}{\xi}\tanh\left(\frac{\xi t_6(\mathbf{r})}{t_4(\mathbf{r})}\right)} \tag{3.24}$$

$$t_{\xi,B_{2/1,c}}(\mathbf{r}) = t_0(\mathbf{r}) + t_2(\mathbf{r}) + \frac{t_4(\mathbf{r})}{1 - \frac{\ln 2}{\xi} + \mathrm{softReLU}_\xi\left(-\frac{t_6(\mathbf{r})}{t_4(\mathbf{r})}\right)} \tag{3.25}$$

3.2.2 Meijer-G Resummation

The Borel approach was used to get the hypergeometric resummation of the kinetic energy density's gradient approximation. Following the Borel approach, the coefficients must be divided by $n!$ to reduce the factorial growth of the z_n coefficients, giving:

$$\begin{aligned} b_0(\mathbf{r}) &= \frac{z_0(\mathbf{r})}{0!} = z_0(\mathbf{r}) = 1 \\ b_1(\mathbf{r}) &= \frac{z_1(\mathbf{r})}{1!} = z_1(\mathbf{r}) = \frac{t_2(\mathbf{r})}{t_0(\mathbf{r})} \\ b_2(\mathbf{r}) &= \frac{z_2(\mathbf{r})}{2!} = \frac{z_2(\mathbf{r})}{2} = \frac{t_4(\mathbf{r})}{2t_0(\mathbf{r})} \\ &\vdots \end{aligned} \tag{3.26}$$

For a hypergeometric resummation of order $N = 1$, only one ratio needs to be set equal to a Padé approximant,

$$r(0) = \frac{b_1}{b_0} = \frac{t_2(\mathbf{r})}{t_0(\mathbf{r})} = \frac{p_0}{1} = p_0. \tag{3.27}$$

The solution of the polynomials is empty, so the resulting hypergeometric vectors are $\mathbf{x} = \{1\}$ and $\mathbf{y} = \{\}$. The resulting

$$t_{MG_1} = t_0 \, G^{2,1}_{1,2}\left(\begin{matrix} 1 \\ 1,1 \end{matrix} \middle| -\frac{t_0}{t_2} \right) \tag{3.28}$$

The expression for the Meijer-G approximant of the kinetic energy density

expansion for order $N = 2$ is given by:

$$t_{MG_2} = t_0 + t_2\, G^{2,1}_{1,2}\left(\begin{matrix}1\\1,1\end{matrix}\middle|-\frac{t_2}{t_4}\right) \tag{3.29}$$

This expression is very similar to the the first order Meijer-G function. This is the result of the additional step, describe previously, that transforms an even order into an odd order Meijer-G function. For $N = 3$, we have

$$t_{MG_3} = t_0 \frac{\Gamma\left(\frac{p_0}{p_1}\right)}{\Gamma\left(\frac{1}{q_1}\right)} G^{3,1}_{2,3}\left(\begin{matrix}1,\frac{1}{q_1}\\1,1,\frac{p_0}{p_1}\end{matrix}\middle|-\frac{q_1}{p_1}\right) \tag{3.30}$$

where $p_0 = \frac{t_2}{t_0}$, $p_1 = \frac{t_0 t_4 t_6 + 3t_2 t_4^2 - 4t_2^2 t_6}{4t_0 t_2 t_6 - 6t_0 t_4^2}$, and $q_1 = \frac{3t_0 t_4^2 - t_0 t_2 t_6 - 3t_2^2 t_4}{2t_0 t_2 t_6 - 3t_0 t_4^2}$. To remove singularities, the ReLU function is also used.

$$t_{MG_{1,a}} = -t_0\, \text{softReLU}_\xi\left(\frac{t_0}{t_2}\right)\, \text{U}\left(1, 1, -\frac{t_0}{t_2}\right) \tag{3.31}$$

$$t_{MG_{1,b}} = t_0\left(0.5 + \text{ softReLU}_\xi\left(\frac{t_0}{t_2} - 0.5\right)\right)\, \text{U}\left(1, 1, -0.5 - \text{ softReLU}_\xi\left(\frac{t_0}{t_2} - 0.5\right)\right) \tag{3.32}$$

where $U(1, 1, z) = \int_0^\infty \frac{e^{-zt}}{1+t}\, \mathrm{d}t$ is the Tricomi confluent hypergeometric function. For the second order Meijer-G, introducing an activation function gives the

following expression:

$$
\begin{aligned}
t_{MG_{2,a}} = t_0 \left[0.5 + \ \mathrm{softReLU}_\xi \left(\frac{t_2}{t_4} - 0.5\right)\right] \ \mathrm{U}\left(1, 1, -0.5 - \ \mathrm{softReLU}_\xi \left(\frac{t_2}{t_4} - 0.5\right)\right) \\
+ \left(t_2 \ \left[-0.5 - \mathrm{softReLU}_\xi \left(\frac{t_2}{t_4} - 0.5\right)\right]^2 - 0.5 - \mathrm{softReLU}_\xi \left(\frac{t_2}{t_4} - 0.5\right)\right) \\
\times \mathrm{U}\left(2, 2, -0.5 - \ \mathrm{softReLU}_\xi \left(\frac{t_2}{t_4} - 0.5\right)\right) \qquad (3.33)
\end{aligned}
$$

Chapter 4

Results and Discussion

4.1 Results and Discussion

The noninteracting kinetic energy was evaluated for the the atoms H-Ar and the molecules H_2, HF, LiH, LiF, N_2, H_2O, NH_3, and CH_4. The calculation was performed using Gaussian 16 with two different methods UHF/UGBS and UPBEPBE/UGBS. These calculated kinetic energies will be considered exact; they are exact except for basis-set truncation error, which we believe to be negligible compared to the errors in the kinetic-energy functional for these very large basis sets. For the functionals that had parameters, we used the atoms to determine the parameter in the kinetic energy functionals and the molecules to test the accuracy of the model. The average of the errors for the non-parameterized functionals was also computed, so that comparisons with the fitted data could be made.

The mean, mean absolute, minimum and maximum percentage error are obtained for each functional and method. Tables A.1 and A.2 are the results of only taking the molecules of the set, and Tables A.3 and A.4 summarize the percentage errors for all species considered, but do not include the fitted functionals.

The truncated gradient expansion kinetic energy density functionals give very similar results whether or not the extra terms that integrate to zero are included. For example, in Table A.1, $t_0 + t_2$ and $t_0 + t_{2j}$ give the exact same numbers for the mean percentage error. This is expected since the only differences between these functionals is the integration error associated with the numerical integration of a term that analytically integrates to zero. Nonetheless, the resummation results can vary greatly when including or excluding these terms. For example, in Table A.1 one notes that for the functionals $t_{MG_{2,a}}$ and $t_{MG_{2j,a}}$ differ by 2 orders of magnitude, even though they differ only by whether the zero-integrating terms are included or not. This is likely due to the behaviour of the kinetic energy densities near the nuclei, which are very different. (Figure 4.1 shows how different t_4 and t_{4j} plots are for the Be atom.) These fluctuations significantly affect the kinetic energy density estimation because of the mathematical expressions of each functional.

It is also worth noting that the results for the sixth-order gradient expansion,

$t_0 + t_2 + t_4 + t_6$, clearly show that the series diverges. The simple truncated gradient expansion that gives the best result is $t_0 + t_2$. This is normal since t_4 and t_6 diverge near the nucleus far from the systems, as shown in Figure 3.2. It is also not surprising, that $t_{B_{2/1}}$, from Ref. [23], yields such low percentage errors. This functional requires calculation of t_6, meaning it is computationally costly.

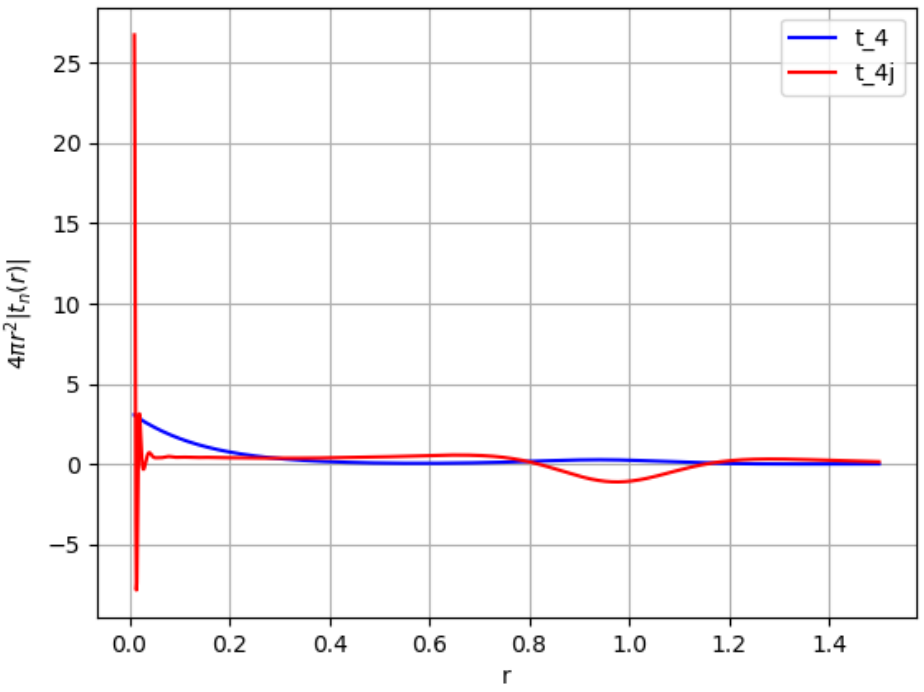

Figure 4.1: Plots of the radial distribution of the kinetic energy densities t_4 and t_{4j} of Be atom. Although the extra terms on $t_4 j$ integrate to zero, the behaviour of the function is very different.

Overall, the gap between using UHF/UGBS and UPBEPBE/UGBS gener-

ated density matrices for the evaluation of the functionals is not significant and no noticeable trend was determined. Tables A.3 and A.4 does not include the fitted functionals because these numbers were calculated for the complete set. These numbers are more reliable when comparing only non-parameterized functionals. The only functional that gives better average accuracy than t_0+t_2 is $t_{B_{2/1}}$. Some of the other functionals are relatively good, however, namely, $t_{B_{0/1}}$, $t_{B_{1/1j}}$, t_{MG_1}, t_{MG_2}, and t_{MG_2j}.

Looking at Table A.1 and A.2, the parameterized functionals that give percentage errors comparable to $t_0 + t_2$ kinetic energy functional are: $t_{B_{0/1j,a}}$, $t_{B_{0/1,c}}$, $t_{B_{0/1,e}}$, $t_{B_{1/1,a}}$, $t_{B_{1/1j,a}}$, $t_{B_{1/1,b}}$, $t_{B_{1/1j,b}}$, $t_{B_{1/1,c}}$, and $t_{B_{1/1j,c}}$. The fitting does improve the accuracy of the kinetic energy evaluation if it is compared to their respective original expressions, but fitting does not guarantee better results, for example, the Meijer-G approximants. This suggests that in the Meijer-G functionals, the parameter values that are appropriate for atoms (used as training data) are inappropriate for molecules (used as testing data). Based on the results for the parameterized functionals, it would be interesting to extend this study to include heavier atoms and molecules that are larger, or which contain heavier atoms. However, since the worst results are usually associated with the 2-electron Hydrogen molecule (where, incidentally, the Weizsäcker functional is exact), it seems likely that our results would only improve for larger molecular systems.

Table 4.1: Mean, mean absolute, minimum and maximum percentage error of the kinetic energy of each functional with UHF/UGBS being the reference. Only the molecules of the set were considered. The fitting was done with atoms H-Ar.

Functional	Mean	Mean Abs.	Min		Max	
t_0	-7.35	9.39	LiH	-13.9	H_2	8.18
$t_0 + t_2$	2.1	3.54	LiH	-3.67	H_2	21.95
$t_0 + t_2 + t_4$	4.28	4.65	LiH	-1.17	H_2	26.49
$t_0 + t_2 + t_4 + t_6$	-7.44×10^5	744×10^5	H_2	-4.50×10^6	CH_4	-2.81×10^4
$t_0 + t_{2j}$	2.1	3.54	LiH	-3.67	H_2	21.95
$t_0 + t_{2j} + t_{4j}$	3.65	4.46	LiH	-1.64	H_2	26.5
$t_{B_{1/1}}$	4.2	4.89	LiH	-1.98	H_2	21.62
$t_{B_{1/1j}}$	3.1	4.05	LiH	-2.67	H_2	18.3
$t_{B_{0/1}}$	4.3	4.43	LiF	-0.51	H_2	24.99
$tB_{0/1j}$	-26.59	142.2	N_2	-423.51	H_2	425.18
$t_{B_{2/1}}$	2.29	3.98	LiH	-3.08	H_2	21.49
t_{MG_1}	5.12	5.5	LiH	-1.54	H_2	22.85
$t_{MG_{1j}}$	-24.86	24.86	LiH	-29.8	H_2	-18.03
t_{MG_2}	3.12	4.04	LiH	-2.67	H_2	23.29
$t_{MG_{2j}}$	3.16	4.07	LiH	-2.48	H_2	22.9
$t_{\xi,B_{0/1,a}}$	-2.42	6.3	LiH	-8.51	H_2	15.5
$t_{\xi,B_{0/1j,a}}$	-0.26	3.47	LiH	-8.44	H_2	12.84
$t_{\xi,B_{0/1,b}}$	-5.59	8.11	LiH	-12.17	H_2	10.09
$t_{\xi,B_{0/1j,b}}$	-7.35	9.39	LiH	-13.91	H_2	8.18
$t_{\xi,B_{0/1,c}}$	0.58	3.56	LiH	-6.21	H_2	16.56
$t_{\xi,B_{0/1j,c}}$	-6.67	9.29	NH_3	-13.71	H_2	10.49
$t_{\xi,B_{0/1,d}}$	-25.74	25.74	LiH	-30.58	H_2	-13.73
$t_{\xi,B_{0/1j,d}}$	-54.89	54.89	N_2	-58.81	H_2	-47.29
$t_{\xi,B_{0/1,e}}$	2.39	3.65	LiH	-3.69	H_2	20.98
$t_{\xi,B_{0/1j,e}}$	-2.91	5.31	LiH	-10.1	H_2	9.58
$t_{\xi,B_{0/1,f}}$	-1.64	5.75	LiH	-6.74	H_2	16.42
$t_{\xi,B_{0/1j,f}}$	-22.5	22.5	LiH	-27.83	H_2	-8.62
$t_{\xi,B_{1/1,a}}$	-0.06	4.72	LiH	-6.13	H_2	18.64
$t_{\xi,B_{1/1j,a}}$	0.51	4.19	LiH	-5.76	H_2	18.78
$t_{\xi,B_{1/1,b}}$	2.76	3.83	LiH	-2.95	H_2	22.85
$t_{\xi,B_{1/1j,b}}$	2.61	3.64	LiH	-2.73	H_2	22.03
$t_{\xi,B_{1/1,c}}$	2.99	4.03	LiH	-1.98	H_2	23.33
$t_{\xi,B_{1/1j,c}}$	3.88	4.99	LiH	-3.0	H_2	21.37
$t_{MG_{1,a}}$	5.24	5.56	LiH	-1.27	H_2	23.5
$t_{MG_{1,b}}$	-205.29	205.29	H_2	-223.77	LiH	-198.84
$t_{MG_{1j,b}}$	-144.18	144.18	HF	-147.48	N_2	-140.18
$t_{MG_{2,a}}$	-1976.97	1976.97	H_2	-1.24×10^4	LiF	-286.0
$t_{MG_{2j,a}}$	72.2	299.87	H_2	-779.86	LiH	720.73

Table 4.2: Mean, mean absolute, minimum and maximum percentage error of the kinetic energy of each functional with UPBEPBE/UGBS being the reference. Only the molecules of the set were considered. The fitting was done with atoms H-Ar.

Functional	Mean	Mean Abs.	min		max	
t_0	-8.39	9.07	LiH	-14.2	H_2	2.69
$t_0 + t_2$	0.94	3.03	LiH	-3.97	H_2	15.9
$t_0 + t_2 + t_4$	3.05	3.57	LiH	-1.56	H_2	20.09
$t_0 + t_2 + t_4 + t_6$	-320×10^5	3.20×10^5	H_2	-1.95×10^6	LiF	-224.38
$t_0 + t_{2j}$	0.95	3.03	LiH	-3.97	H_2	15.9
$t_0 + t_{2j} + t_{4j}$	2.42	3.48	LiH	-2.01	H_2	20.12
$t_{B_{1/1}}$	3.67	4.61	LiH	-2.34	H_2	21.75
$t_{B_{1/1j}}$	2.33	3.26	LiH	-2.32	H_2	14.36
$t_{B_{0/1}}$	4.0	4.41	LiH	-1.14	H_2O	15.64
$t_{B_{0/1j}}$	-68.77	68.77	H_2	-167.69	CH_4	-7.51
$t_{B_{2/1}}$	0.99	3.15	LiH	-3.72	H_2	14.82
t_{MG_1}	4.02	4.42	LiH	-1.62	H_2	16.98
$t_{MG_{1j}}$	-25.66	25.66	LiH	-30.22	H_2	-22.59
t_{MG_2}	1.95	2.99	LiH	-2.97	H_2	17.17
$t_{MG_{2j}}$	1.93	2.99	LiH	-2.85	H_2	16.6
$t_{\xi,B_{0/1,a}}$	-382.06	382.06	H_2	-475.87	LiF	-364.39
$t_{\xi,B_{0/1j,a}}$	-1.01	2.94	LiH	-8.27	H_2	7.74
$t_{\xi,B_{0/1,b}}$	-6.64	7.77	LiH	-12.43	H_2	4.55
$t_{\xi,B_{0/1j,b}}$	-8.4	9.07	LiH	-14.2	H_2	2.68
$t_{\xi,B_{0/1,c}}$	-0.48	3.16	LiH	-6.47	H_2	10.72
$t_{\xi,B_{0/1j,c}}$	-10.52	10.52	N2	-16.66	H_2	-0.93
$t_{\xi,B_{0/1,d}}$	-26.58	26.58	LiH	-30.82	H_2	-18.09
$t_{\xi,B_{0/1j,d}}$	-55.87	55.87	N2	-59.4	H_2O	-51.28
$t_{\xi,B_{0/1,e}}$	1.57	2.78	LiH	-3.46	H_2	15.81
$t_{\xi,B_{0/1j,e}}$	-3.71	4.83	LiH	-10.08	H_2	4.46
$t_{\xi,B_{0/1,f}}$	4.66	7.37	LiH	-2.94	H_2	48.11
$t_{\xi,B_{0/1j,f}}$	-38.65	39.8	H_2O	-218.09	H_2	4.6
$t_{\xi,B_{1/1,a}}$	-1.2	4.37	LiH	-6.43	H_2	12.65
$t_{\xi,B_{1/1j,a}}$	-0.64	3.82	LiH	-6.01	H_2	12.74
$t_{\xi,B_{1/1,b}}$	1.73	2.86	LiH	-3.1	H_2	16.95
$t_{\xi,B_{1/1j,b}}$	1.39	2.62	LiH	-3.1	H_2	15.78
$t_{\xi,B_{1/1,c}}$	1.85	2.91	LiH	-2.89	H_2	17.23
$t_{\xi,B_{1/1j,c}}$	1.72	2.82	LiH	-2.93	H_2	16.6
$t_{MG_{1,a}}$	4.13	4.47	LiH	-1.38	H_2	17.58
$t_{MG_{1,b}}$	-204.17	204.17	H_2	-217.83	LiH	-198.73
$t_{MG_{1j,b}}$	-144.75	144.75	HF	-147.39	NH_3	-142.41
$t_{MG_{2,a}}$	-1992.08	1992.08	H_2	-1.24×10^4	HF	-326.27
$t_{MG_{2j,a}}$	488.88	567.2	H_2	-289.56	LiH	3116.61

Table 4.3: Mean, mean absolute, minimum and maximum percentage error of the kinetic energy of each functional with UHF/UGBS being the reference.

Functional	Mean	Mean Abs.	min		max	
t_0	-8.16	8.79	LiH	-13.9	H_2	8.18
$t_0 + t_2$	0.62	1.5	LiH	-3.67	H_2	21.95
$t_0 + t_2 + t_4$	2.58	2.69	LiH	-1.17	H_2	26.49
$t_0 + t_2 + t_4 + t_6$	-4.35 $\times 10^1 4$	$4.35 \times 10^1 4$	O	$-1.13 \times 10^1 6$	Mg	-132.54
$t_0 + t_{2j}$	0.64	1.49	LiH	-3.67	H_2	21.95
$t_0 + t_{2j} + t_{4j}$	3.77	4.17	LiH	-1.64	O	50.38
$t_{B_{1/1}}$	1.12	3.84	Be	-15.95	H_2	21.62
$t_{B_{1/1j}}$	1.71	2.05	LiH	-2.67	H_2	18.3
$t_{B_{0/1}}$	3.0	3.04	LiF	-0.51	H_2	24.99
$tB_{0/1j}$	-62.53	181.57	Cl	-1258.28	He	502.85
$t_{B_{2/1}}$	0.39	2.89	He	-12.68	H_2	21.49
t_{MG_1}	3.27	3.38	LiH	-1.54	H_2	22.85
$t_{MG_{1j}}$	-23.39	23.39	LiH	-29.8	Ar	-16.6
t_{MG_2}	1.55	1.83	LiH	-2.67	H_2	23.29
$t_{MG_{2j}}$	1.57	1.84	LiH	-2.48	H_2	22.9

Table 4.4: Mean, mean absolute, minimum and maximum percentage error of the kinetic energy of each functional with UPBEPBE/UGBS being the reference.

Functional	Mean	Mean Abs.	min		max	
t_0	-8.63	8.84	LiH	-14.2	H_2	2.69
$t_0 + t_2$	0.1	1.34	LiH	-3.97	H_2	15.9
$t_0 + t_2 + t_4$	1.97	2.12	LiH	-1.56	H_2	20.09
$t_0 + t_2 + t_4 + t_6$	-1.15×10^9	1.15×10^9	Li	-2.81×10^{10}	S	3.45×10^4
$t_0 + t_{2j}$	0.11	1.33	LiH	-3.97	H_2	15.9
$t_0 + t_{2j} + t_{4j}$	1.26	1.79	LiH	-2.01	H_2	20.12
$t_{B_{1/1}}$	-29.64	34.67	He	-684.54	H_2	21.75
$t_{B_{1/1j}}$	1.27	1.6	LiH	-2.32	H_2	14.36
$t_{B_{0/1}}$	2.02	2.57	He	-4.77	H_2O	15.64
$t_{B_{0/1j}}$	91.85	227.63	He	-210.85	P	3619.33
$t_{B_{2/1}}$	0.31	2.38	H	-7.08	H_2	14.82
t_{MG_1}	2.8	2.93	LiH	-1.62	H_2	16.98
$t_{MG_{1j}}$	-23.68	23.68	LiH	-30.22	Ar	-16.4
t_{MG_2}	1.02	1.34	LiH	-2.97	H_2	17.17
$t_{MG_{2j}}$	0.99	1.32	LiH	-2.85	H_2	16.6

Chapter 5

Conclusions

5.1 Conclusions

As expected, the second-order Pade approximant, $t_0 + t_2$, and the $t_{B_{2/1}}$ Padé approximant give good results. However, the $t_0 + t_2$ functional is more affordable to evaluate since it only requires two terms in the gradient expansion, and the difference in quality between these two functionals is not very large. The functionals $t_{B_{0/1}}$, $t_{B_{1/1j}}$, t_{MG_1}, t_{MG_2}, and t_{MG_2j} also gave relatively good results, but not better than the simple second-order gradient expansion, t_0+t_2. Some parameterized functionals, namely, $t_{B_{0/1j,a}}$, $t_{B_{0/1,c}}$, $t_{B_{0/1,e}}$, $t_{B_{1/1,a}}$, $t_{B_{1/1j,a}}$, $t_{B_{1/1,b}}$, $t_{B_{1/1j,b}}$, $t_{B_{1/1,c}}$, and $t_{B_{1/1j,c}}$ give a low percentage error, though often with larger mean errors (indicating a systematic bias).

Two functionals,$t_{B_{0/1,c}}$ and $t_{B_{1/1j,a}}$, performed better than $t_0 + t_2$. They have

similar expressions, and the first one only requires kinetic energy density terms up to second order. Aside from the fitting, the evaluation of $t_{B_{0/1,c}}$ and $t_0 + t_2$ would have similar computational cost. This functional would seem promising, but a closer look at the behaviour of the expression, the low yield is a result of a fortuitous cancellation of error. The functional does not recover the original Padé functional at any value, and because there is no restriction on the values or the argument of the hyperbolic tangent function, the evaluation yields negative values, that compensate for the overestimation at other points of the molecular space.

Overall, even the best functionals have errors that are about three orders of magnitude larger than is acceptable, since quantitative quantum chemistry calculations require mean-absolute-errors of 10^{-3} a.u. We can only conclude that the gradient expansion diverges too strongly for the resummation techniques we have considered here to be effective. Since higher-order terms in the gradient expansion are unlikely to be practical to compute, and are likely to be extremely sensitive to basis-set convergence errors, including higher-order terms is unlikely to be beneficial. However, if one could mathematically characterize key features of the exact gradient expansion (including, for example, the location and type of the singularities that are closest to the original and/or the asymptotic form of the gradient expansion for the rapidly-varying uniform-electron-gas limit), one could select a function that is more suitable than either the Padé or the Meijer-G form. If such a form were known, one might plausibly parameterize the form using low-order terms in the gradient expansion and obtain a functional that would exceed the performance of those

considered here. Failing that, one may only hope that one could find functionals that, while far from universal, were nonetheless adequate for certain classes of molecular systems and their reactions. Finding functionals which, while far from universal, are nonetheless effective for specific chemical applications is a challenging topic for future work.

Appendix A

Detailed Results

Table A.1: Mean, mean absolute, minimum and maximum percentage error of the kinetic energy of each functional with UHF/UGBS being the reference. Only the molecules of the set were considered. The fitting was done with atoms H-Ar.

Functional	ξ	Mean	Min.		Max.		Mean Abs.	Min. Abs.		Max. Abs.	
t_0		-7.35	LiH	-13.9	H_2	8.18	9.39	H_2	8.18	LiH	13.9
$t_0 + t_2$		2.1	LiH	-3.67	H_2	21.95	3.54	CH_4	0.02	H_2	21.95
$t_0 + t_{2j}$		2.1	LiH	-3.67	H_2	21.95	3.54	CH_4	0.02	H_2	21.95
$t_0 + t_2 + t_4$		4.28	LiH	-1.17	H_2	26.49	4.65	LiF	0.3	H_2	26.49
$t_0 + t_{2j} + t_{4j}$		3.65	LiH	-1.64	H_2	26.5	4.46	HF	0.02	H_2	26.5
$t_0 + t_2 + t_4 + t_6$		-7.44×10^5	H_2	-4.50×10^6	CH_4	-28056.36	7.44×10^5	CH_4	28056.36	H_2	4.50×10^6
$t_{B_{0/1}}$		4.3	LiF	-0.51	H_2	24.99	4.43	LiF	0.51	H_2	24.99
$t_{B_{0/1j}}$		-26.59	N_2	-423.51	H_2	425.18	142.2	HF	21.84	H_2	425.18
$t_{B_{1/1}}$		4.2	LiH	-1.98	H_2	21.62	4.89	H_2O	0.09	H_2	21.62
$t_{B_{1/1j}}$		3.1	LiH	-2.67	H_2	18.3	4.05	HF	0.53	H_2	18.3
$t_{B_{2/1}}$		2.29	LiH	-3.08	H_2	21.49	3.98	HF	0.25	H_2	21.49
$t_{B_{1/2}}$		4.73	LiF	-0.44	H_2	25.4	4.85	H_2O	0.03	H_2	25.4
t_{MG_1}		5.12	LiH	-1.54	H_2	22.85	5.5	LiF	1.35	H_2	22.85
$t_{MG_{1j}}$		-24.86	LiH	-29.8	H_2	-18.03	24.86	H_2	18.03	LiH	29.8
t_{MG_2}		3.12	LiH	-2.67	H_2	23.29	4.04	HF	0.7	H_2	23.29
$t_{MG_{2j}}$		3.16	LiH	-2.48	H_2	22.9	4.07	HF	0.54	H_2	22.9
$t_{\xi,B_{0/1,a}}$	~ 1	-361.9	H_2	-428.71	H_2O	-254.38	361.9	H_2O	254.38	H_2	428.71
$t_{\xi,B_{0/1j,a}}$	1.16	-0.26	LiH	-8.44	H_2	12.84	3.47	HF	0.29	H_2	12.84
$t_{\xi,B_{0/1,b}}$	~ 1	-5.59	LiH	-12.17	H_2	10.09	8.11	HF	6.69	LiH	12.17
$t_{\xi,B_{0/1j,b}}$	190.17	-7.35	LiH	-13.91	H_2	8.18	9.39	H_2	8.18	LiH	13.91
$t_{\xi,B_{0/1,c}}$	1.24	0.58	LiH	-6.21	H_2	16.56	3.56	N_2	0.43	H_2	16.56
$t_{\xi,B_{0/1j,c}}$	1.65	-6.67	NH_3	-13.71	H_2	10.49	9.29	H_2O	0.37	NH_3	13.71
$t_{\xi,B_{0/1,d}}$	~ 1	-25.74	LiH	-30.58	H_2	-13.73	25.74	H_2	13.73	LiH	30.58
$t_{\xi,B_{0/1j,d}}$	~ 1	-54.89	N_2	-58.81	H_2	-47.29	54.89	H_2	47.29	N_2	58.81
$t_{\xi,B_{0/1,e}}$	2.97	2.39	LiH	-3.69	H_2	20.98	3.65	HF	0.33	H_2	20.98
$t_{\xi,B_{0/1j,e}}$	3.07	-2.91	LiH	-10.1	H_2	9.58	5.31	HF	2.65	LiH	10.1
$t_{\xi,B_{0/1,f}}$	2.72	-1.64	LiH	-6.74	H_2	16.42	5.75	N_2	3.24	H_2	16.42
$t_{\xi,B_{0/1j,f}}$	1.16	-1.13	H_2O	-65.05	HF	91.99	30.28	CH_4	8.29	HF	91.99
$t_{\xi,B_{1/1,a}}$	~ 1	-0.06	LiH	-6.13	H_2	18.64	4.72	N_2	1.51	H_2	18.64
$t_{\xi,B_{1/1j,a}}$	~ 1	0.51	LiH	-5.76	H_2	18.78	4.19	N_2	0.51	H_2	18.78
$t_{\xi,B_{1/1,b}}$	8.15	2.76	LiH	-2.95	H_2	22.85	3.83	HF	0.35	H_2	22.85
$t_{\xi,B_{1/1j,b}}$	3.59	2.61	LiH	-2.73	H_2	22.03	3.64	HF	0.25	H_2	22.03
$super_2$		1.84	LiH	-4.03	H_2	20.48	3.41	H_2O	0.02	H_2	20.48
$super_4$		2.95	LiH	-2.87	H_2	21.92	3.92	HF	0.7	H_2	21.92
$super_6$		4.01	LiH	-1.72	H_2	23.36	4.47	LiF	0.11	H_2	23.36
$super_{2j}$		-28.0	LiH	-35.19	H_2O	-23.46	28.0	H_2O	23.46	LiH	35.19
$super_{4j}$		-29.61	LiH	-36.99	H_2O	-24.64	29.61	H_2O	24.64	LiH	36.99
$logit_{t2}$	~ 1	-7.06	LiH	-13.05	H_2	8.28	9.13	N_2	8.2	LiH	13.05
$logit_{t2j}$	~ 1	0.92	LiH	-10.61	H_2	6.73	3.98	LiF	1.44	LiH	10.61
$logit_{t4}$	~ 1	-6.79	LiH	-12.77	H_2	8.28	8.86	N_2	7.87	LiH	12.77
$logit_{t4j}$	~ 1	1.02	LiH	-10.48	H_2	6.91	4.01	LiF	1.45	LiH	10.48
$logit_{t6}$	~ 1	-6.66	LiH	-12.8	H_2	8.2	8.71	N_2	7.67	LiH	12.8
$logit_{B_{0/1}}$	~ 1	-7.05	LiH	-13.03	H_2	8.27	9.12	N_2	8.18	LiH	13.03
$logit_{B_{0/1j}}$	5.92	-19.57	NH_3	-93.41	H_2O	53.31	35.79	LiF	1.72	NH_3	93.41
$logit_{B_{1/1}}$	~ 1	-7.06	LiH	-13.05	H_2	8.27	9.13	N_2	8.19	LiH	13.05
$logit_{B_{1/1j}}$	~ 1	0.92	LiH	-10.61	H_2	6.72	3.98	LiF	1.45	LiH	10.61
$logit_{B_{2/1}}$	~ 1	-6.28	LiH	-12.62	H_2	8.27	8.35	N_2	6.69	LiH	12.62
$t_{\xi,B_{1/1,c}}$	~ 1	3.02	LiH	-2.59	H_2	23.33	3.95	HF	0.53	H_2	23.33
$t_{\xi,B_{1/1j,c}}$	2.01	2.74	LiH	-2.79	H_2	22.43	3.78	HF	0.34	H_2	22.43
$t_{\xi,B_{1/1,d}}$	~ 1	2.99	LiH	-1.98	H_2	23.33	4.03	HF	0.32	H_2	23.33
$t_{\xi,B_{1/1j,d}}$	~ 1	3.88	LiH	-3.0	H_2	21.37	4.99	HF	0.35	H_2	21.37
$t_{\xi,B_{2/1,a}}$	~ 1	2.12	LiH	-3.66	H_2	21.82	3.55	H_2O	0.02	H_2	21.82
$t_{\xi,B_{2/1,b}}$	51.64	4.07	LiH	-1.35	H_2	25.1	4.48	LiF	0.31	H_2	25.1
$t_{\xi,B_{2/1,c}}$	1682.70	3.03	LiH	-2.66	H_2	23.45	3.97	HF	0.55	H_2	23.45
$t_{MG_{1,a}}$	~ 1	5.24	LiH	-1.27	H_2	23.5	5.56	LiH	1.27	H_2	23.5
$t_{MG_{1,b}}$	~ 1	-205.29	H_2	-223.77	LiH	-198.84	205.29	LiH	198.84	H_2	223.77
$t_{MG_{1j,b}}$	442.70	-144.18	HF	-147.48	N_2	-140.18	144.18	N_2	140.18	HF	147.48
$t_{MG_{2,a}}$	185.85	-1976.97	H_2	-12398.58	LiF	-286.0	1976.97	LiF	286.0	H_2	12398.58
$t_{MG_{2j,a}}$	360.77	72.2	H_2	-779.86	LiH	720.73	299.87	H_2O	30.92	H_2	779.86

Table A.2: Mean, mean absolute, minimum and maximum percentage error of the kinetic energy of each functional with UPBEPBE/UGBS being the reference. Only the molecules of the set were considered. The fitting was done with atoms H-Ar.

Functional	ξ	Mean	Min.		Max.		Mean Abs.	Min. Abs.		Max. Abs.	
t_0		-8.39	LiH	-14.2	H_2	2.69	9.07	H_2	2.69	LiH	14.2
$t_0 + t_2$		0.94	LiH	-3.97	H_2	15.9	3.03	N_2	0.26	H_2	15.9
$t_0 + t_{2j}$		0.95	LiH	-3.97	H_2	15.9	3.03	N_2	0.25	H_2	15.9
$t_0 + t_2 + t_4$		3.05	LiH	-1.56	H_2	20.09	3.57	LiF	0.51	H_2	20.09
$t_0 + t_{2j} + t_{4j}$		2.42	LiH	-2.01	H_2	20.12	3.48	H_2O	0.4	H_2	20.12
$t_0 + t_2 + t_4 + t_6$		-3.20×10^5	H_2	-1.95×10^6	LiF	-224.38	3.20×10^5	LiF	224.38	H_2	1.954×10^6
$t_{B_{0/1}}$		4.0	LiH	-1.14	H_2O	15.64	4.41	LiF	0.49	H_2O	15.64
$t_{B_{0/1j}}$		-68.77	H_2	-167.69	CH_4	-7.51	68.77	CH_4	7.51	H_2	167.69
$t_{B_{1/1}}$		3.67	LiH	-2.34	H_2	21.75	4.61	H_2O	0.55	H_2	21.75
$t_{B_{1/1j}}$		2.33	LiH	-2.32	H_2	14.36	3.26	HF	0.42	H_2	14.36
$t_{B_{2/1}}$		0.99	LiH	-3.72	H_2	14.82	3.15	CH_4	0.07	H_2	14.82
$t_{B_{1/2}}$		2.05	LiH	-2.87	H_2	13.33	3.07	HF	0.41	H_2	13.33
t_{MG_1}		4.02	LiH	-1.62	H_2	16.98	4.42	LiF	1.15	H_2	16.98
$t_{MG_{1j}}$		-25.66	LiH	-30.22	H_2	-22.59	25.66	H_2	22.59	LiH	30.22
t_{MG_2}		1.95	LiH	-2.97	H_2	17.17	2.99	HF	0.32	H_2	17.17
$t_{MG_{2j}}$		1.93	LiH	-2.85	H_2	16.6	2.99	HF	0.15	H_2	16.6
$t_{\xi,B_{0/1,a}}$	~ 1	-382.06	H_2	-475.87	LiF	-364.39	382.06	LiF	364.39	H_2	475.87
$t_{\xi,B_{0/1j,a}}$	1.16	-1.01	LiH	-8.27	H_2	7.74	2.94	HF	0.45	LiH	8.27
$t_{\xi,B_{0/1,b}}$	~ 1	-6.64	LiH	-12.43	H_2	4.55	7.77	H_2	4.55	LiH	12.43
$t_{\xi,B_{0/1j,b}}$	189.79	-8.4	LiH	-14.2	H_2	2.68	9.07	H_2	2.68	LiH	14.2
$t_{\xi,B_{0/1,c}}$	1.24	-0.48	LiH	-6.47	H_2	10.72	3.16	HF	0.91	H_2	10.72
$t_{\xi,B_{0/1j,c}}$	1.63	-10.52	N_2	-16.66	H_2	-0.93	10.52	H_2	0.93	N_2	16.66
$t_{\xi,B_{0/1,d}}$	~ 1	-26.58	LiH	-30.82	H_2	-18.09	26.58	H_2	18.09	LiH	30.82
$t_{\xi,B_{0/1j,d}}$	~ 1	-55.87	N_2	-59.4	H_2O	-51.28	55.87	H_2O	51.28	N_2	59.4
$t_{\xi,B_{0/1,e}}$	2.52	1.57	LiH	-3.46	H_2	15.81	2.78	HF	0.13	H_2	15.81
$t_{\xi,B_{0/1j,e}}$	3.10	-3.71	LiH	-10.08	H_2	4.46	4.83	HF	2.79	LiH	10.08
$t_{\xi,B_{0/1,f}}$	30.85	4.66	LiH	-2.94	H_2	48.11	7.37	N_2	0.69	H_2	48.11
super_2		0.7	LiH	-4.31	H_2	14.53	2.93	N_2	0.27	H_2	14.53
super_4		1.79	LiH	-3.16	H_2	15.91	2.88	HF	0.32	H_2	15.91
super_6		2.83	LiH	-2.01	H_2	17.3	3.41	LiF	0.31	H_2	17.3
super_{2j}		-28.65	LiH	-35.27	H_2O	-23.61	28.65	H_2O	23.61	LiH	35.27
super_{4j}		-30.27	LiH	-37.12	H_2O	-24.81	30.27	H_2O	24.81	LiH	37.12
$logit_{t2}$	~ 1	-8.12	LiH	-13.34	H_2	2.78	8.81	H_2	2.78	LiH	13.34
$logit_{t2j}$	~ 1	-0.04	LiH	-10.82	HF	3.46	3.07	LiF	1.27	LiH	10.82
$logit_{t4}$	~ 1	-7.84	LiH	-13.06	H_2	2.79	8.54	H_2	2.79	LiH	13.06
$logit_{t4j}$	~ 1	0.06	LiH	-10.69	HF	3.46	3.09	LiF	1.27	LiH	10.69
$logit_{t6}$	~ 1	-7.7	LiH	-13.08	H_2	2.76	8.39	H_2	2.76	LiH	13.08
$logit_{B_{0/1}}$	~ 1	-8.11	LiH	-13.33	H_2	2.77	8.8	H_2	2.77	LiH	13.33
$logit_{B_{0/1j}}$	~ 1	-60.73	H_2O	-248.86	H_2	1.36	61.07	H_2	1.36	H_2O	248.86
$logit_{B_{1/1}}$	~ 1	-8.12	LiH	-13.35	H_2	2.77	8.81	H_2	2.77	LiH	13.35
$logit_{B_{1/1j}}$	~ 1	-0.04	LiH	-10.81	HF	3.46	3.06	LiF	1.27	LiH	10.81
$logit_{B_{2/1}}$	~ 1	-7.35	LiH	-12.88	H_2	2.77	8.04	H_2	2.77	LiH	12.88
$t_{\xi,B_{0/1j,f}}$	~ 1	-38.65	H_2O	-218.09	H_2	4.6	39.8	H_2	4.6	H_2O	218.09
$t_{\xi,B_{1/1,a}}$	~ 1	-1.2	LiH	-6.43	H_2	12.65	4.37	N_2	2.17	H_2	12.65
$t_{\xi,B_{1/1j,a}}$	~ 1	-0.64	LiH	-6.01	H_2	12.74	3.82	N_2	1.18	H_2	12.74
$t_{\xi,B_{1/1,b}}$	6.03	1.73	LiH	-3.1	H_2	16.95	2.86	HF	0.1	H_2	16.95
$t_{\xi,B_{1/1j,b}}$	3.68	1.39	LiH	-3.1	H_2	15.78	2.62	H_2O	0.0	H_2	15.78
$t_{\xi,B_{1/1,c}}$	~ 1	1.85	LiH	-2.89	H_2	17.23	2.91	HF	0.16	H_2	17.23
$t_{\xi,B_{1/1j,c}}$	2.48	1.72	LiH	-2.93	H_2	16.6	2.82	HF	0.07	H_2	16.6
$t_{\xi,B_{1/1,d}}$	~ 1	1.56	LiH	-3.34	H_2	16.95	3.2	HF	0.07	H_2	16.95
$t_{\xi,B_{1/1j,d}}$	1.09	1.53	LiH	-3.17	H_2	15.3	2.84	N_2	0.11	H_2	15.3
$t_{\xi,B_{2/1,a}}$	~ 1	0.95	LiH	-3.95	H_2	15.72	2.97	N_2	0.16	H_2	15.72
$t_{\xi,B_{2/1,b}}$	51.62	2.88	LiH	-1.66	H_2	18.97	3.43	LiF	0.52	H_2	18.97
$t_{\xi,B_{2/1,c}}$	2717.02	1.87	LiH	-2.93	H_2	17.38	2.93	HF	0.18	H_2	17.38
$t_{MG_{1,a}}$	~ 1	4.13	LiH	-1.38	H_2	17.58	4.47	LiF	1.16	H_2	17.58
$t_{MG_{1,b}}$	~ 1	-204.17	H_2	-217.83	LiH	-198.73	204.17	LiH	198.73	H_2	217.83
$t_{MG_{1j,b}}$	472.37	-144.75	HF	-147.39	NH_3	-142.41	144.75	NH_3	142.41	HF	147.39
$t_{MG_{2,a}}$	690.23	-1992.08	H_2	-12435.73	HF	-326.27	1992.08	HF	326.27	H_2	12435.73
$t_{MG_{2j,a}}$	113.39	488.88	H_2	-289.56	LiH	3116.61	567.2	N_2	6.93	LiH	3116.61

Table A.3: Mean, mean absolute, minimum and maximum percentage error of the kinetic energy of each functional with UHF/UGBS being the reference.

Functional	Mean	Min.		Max.		Mean Abs.	Min. Abs.		Max. Abs.	
t_0	-8.16	LiH	-13.9	H_2	8.18	8.79	Ar	7.0	LiH	13.9
$t_0 + t_2$	0.62	LiH	-3.67	H_2	21.95	1.5	B	0.02	H_2	21.95
$t_0 + t_{2j}$	0.64	LiH	-3.67	H_2	21.95	1.49	B	0.01	H_2	21.95
$t_0 + t_2 + t_4$	2.58	LiH	-1.17	H_2	26.49	2.69	LiF	0.3	H_2	26.49
$t_0 + t_{2j} + t_{4j}$	3.77	LiH	-1.64	O	50.38	4.17	HF	0.02	O	50.38
$t_0 + t_2 + t_4 + t_6$	-4.35×10^{14}	O	-1.13×10^{16}	Mg	-132.54	4.35×10^{14}	Mg	132.54	O	1.13×10^{16}
$t_{B_{0/1}}$	3.0	LiF	-0.51	H_2	24.99	3.04	Ar	0.16	H_2	24.99
$t_{B_{0/1j}}$	-62.53	Cl	-1258.28	He	502.85	181.57	Si	13.68	Cl	1258.28
$t_{B_{1/1}}$	1.12	Be	-15.95	H_2	21.62	3.84	H_2O	0.09	H_2	21.62
$t_{B_{1/1j}}$	1.71	LiH	-2.67	H_2	18.3	2.05	Al	0.01	H_2	18.3
$t_{B_{2/1}}$	0.38	He	-12.73	H_2	21.49	2.89	P	0.08	H_2	21.49
$t_{B_{1/2}}$	3.64	He	-7.46	H_2	25.4	4.51	H_2O	0.03	H_2	25.4
t_{MG_1}	3.26	LiH	-1.54	H_2	22.85	3.38	LiF	1.35	H_2	22.85
$t_{MG_{1j}}$	-23.39	LiH	-29.8	Ar	-16.6	23.39	Ar	16.6	LiH	29.8
t_{MG_2}	1.55	LiH	-2.67	H_2	23.29	1.83	Ar	0.15	H_2	23.29
$t_{MG_{2j}}$	1.57	LiH	-2.48	H_2	22.9	1.84	F	0.11	H_2	22.9
$super_2$	0.46	LiH	-4.03	H_2	20.48	1.41	H_2O	0.02	H_2	20.48
$super_4$	1.46	LiH	-2.87	H_2	21.92	1.76	F	0.19	H_2	21.92
$super_6$	2.43	LiH	-1.72	H_2	23.36	2.57	LiF	0.11	H_2	23.36
$super_{2j}$	-25.57	LiH	-35.19	Ar	-13.88	25.57	Ar	13.88	LiH	35.19
$super_{4j}$	-26.75	LiH	-36.99	Ar	-13.93	26.75	Ar	13.93	LiH	36.99

Table A.4: Mean, mean absolute, minimum and maximum percentage error of the kinetic energy of each functional with UPBEPBE/UGBS being the reference.

Functional	Mean	Min.		Max.		Mean Abs.	Min. Abs.		Max. Abs.	
t_0	-8.63	LiH	-14.2	H_2	2.69	8.84	H_2	2.69	LiH	14.2
$t_0 + t_2$	0.1	LiH	-3.97	H_2	15.9	1.34	He	0.13	H_2	15.9
$t_0 + t_{2j}$	0.11	LiH	-3.97	H_2	15.9	1.33	He	0.13	H_2	15.9
$t_0 + t_2 + t_4$	1.97	LiH	-1.56	H_2	20.09	2.12	LiF	0.51	H_2	20.09
$t_0 + t_{2j} + t_{4j}$	1.26	LiH	-2.01	H_2	20.12	1.79	Ne	0.01	H_2	20.12
$t_0 + t_2 + t_4 + t_6$	-1.15×10^{9}	Li	-2.81×10^{10}	S	34463.94	1.15×10^{9}	Mg	151.57	Li	2.81×10^{10}
$t_{B_{0/1}}$	2.02	He	-4.77	H_2O	15.64	2.57	Ar	0.08	H_2O	15.64
$t_{B_{0/1j}}$	91.85	He	-210.85	P	3619.33	227.63	CH_4	7.51	P	3619.33
$t_{B_{1/1}}$	-29.64	He	-684.54	H_2	21.75	34.67	S	0.07	He	684.54
$t_{B_{1/1j}}$	1.27	LiH	-2.32	H_2	14.36	1.6	F	0.0	H_2	14.36
$t_{B_{2/1}}$	0.31	H	-7.08	H_2	14.82	2.38	CH_4	0.07	H_2	14.82
$t_{B_{1/2}}$	2.1	Si	-2.95	H_2	13.33	2.74	H	0.05	H_2	13.33
t_{MG_1}	2.8	LiH	-1.62	H_2	16.98	2.93	LiF	1.15	H_2	16.98
$t_{MG_{1j}}$	-23.68	LiH	-30.22	Ar	-16.4	23.68	Ar	16.4	LiH	30.22
t_{MG_2}	1.02	LiH	-2.97	H_2	17.17	1.34	F	0.04	H_2	17.17
$t_{MG_{2j}}$	0.99	LiH	-2.85	H_2	16.6	1.32	Si	0.02	H_2	16.6
$super_2$	-0.06	LiH	-4.31	H_2	14.53	1.31	Be	0.14	H_2	14.53
$super_4$	0.93	LiH	-3.16	H_2	15.91	1.27	F	0.01	H_2	15.91
$super_6$	1.89	LiH	-2.01	H_2	17.3	2.07	LiF	0.31	H_2	17.3
$super_{2j}$	-25.82	He	-35.27	Ar	-13.82	25.82	Ar	13.82	He	35.27
$super_{4j}$	-27.02	He	-37.19	Ar	-13.88	27.02	Ar	13.88	He	37.19

Table A.5: Percentage error of the kinetic energy of each functional with UHF/UGBS being the reference. Part 1.

Specie	t_0	t_0+t_2	t_0+t_{2j}	$t_0+t_2+t_4$	$t_0+t_{2j}+t_{4j}$	$t_0+t_2+t_4+t_6$	$t_{B_{0/1}}$	$t_{B_{0/1}\mathrm{j}}$	$t_{B_{1/1}}$	$t_{B_{1/1}\mathrm{j}}$	$t_{B_{2/1}}$	$t_{B_{1/2}}$	t_{MG_1}	$t_{MG_1\mathrm{j}}$	t_{MG_2}	$t_{MG_{2j}}$
H	-8.21	2.90	2.90	5.96	6.02	-1.66×10^{6}	15.13	-282.31	3.17	3.82	-2.93	11.36	4.14	-25.84	4.07	3.76
He	-10.52	0.59	0.59	3.55	3.47	-9.60×10^{7}	0.57	502.85	-8.42	0.01	-12.73	-7.46	2.55	-26.42	1.67	1.48
Li	-9.85	0.97	0.97	3.66	3.17	-5.32×10^{8}	9.60	-40.55	3.54	1.23	1.32	10.21	3.01	-26.57	2.01	2.08
Be	-9.91	0.51	0.51	2.84	2.38	-5124.73	5.05	-155.36	-15.95	5.37	8.02	17.74	3.01	-27.15	1.55	1.52
B	-10.01	-0.02	-0.01	2.18	1.21	-21819.81	2.54	-50.01	1.99	1.21	0.58	3.26	2.93	-27.19	1.05	1.05
C	-9.70	-0.19	-0.19	1.84	1.44	-6.96×10^{5}	2.44	-59.53	1.54	1.66	0.40	7.23	2.90	-26.71	0.85	1.20
N	-8.96	0.06	0.07	1.93	1.55	-1.12×10^{6}	2.59	-144.38	2.81	3.07	1.22	3.85	3.00	-24.95	1.04	1.30
O	-9.16	-0.53	-0.52	2.42	50.38	-1.13×10^{16}	1.05	-31.18	-0.94	1.35	-2.30	-0.46	2.70	-25.01	0.43	0.64
F	-8.98	-0.75	-0.74	0.87	-0.52	-1.04×10^{6}	1.08	-37.34	0.56	0.20	-0.79	0.56	2.49	-24.50	0.16	0.11
Ne	-8.39	-0.56	-0.54	0.93	0.19	-8.76×10^{5}	0.43	477.47	6.39	0.63	0.76	1.88	2.47	-22.83	0.32	0.39
Na	-8.07	-0.48	-0.46	0.94	-0.33	-4.13×10^{7}	0.52	-40.77	0.38	0.42	-0.69	0.20	2.30	-21.55	0.35	0.39
Mg	-7.82	-0.44	-0.42	0.91	-0.30	-132.54	0.52	61.15	5.15	0.22	1.13	2.34	2.18	-21.15	0.35	0.23
Al	-7.63	-0.43	-0.40	0.88	-0.43	-641.60	0.53	-63.29	0.54	0.01	-0.49	0.49	2.03	-19.82	0.34	0.34
Si	-7.47	-0.42	-0.39	0.85	-0.43	-1529.76	0.42	-13.68	-1.60	-0.02	-4.95	-2.88	1.90	-19.67	0.32	0.13
P	-7.30	-0.41	-0.38	0.83	0.30	-58883.53	0.38	-258.47	1.01	0.32	-0.08	0.72	1.78	-18.03	0.31	0.24
S	-7.21	-0.45	-0.42	0.76	0.24	-73411.85	0.28	-63.01	0.19	-0.56	-0.80	-0.06	1.63	-18.41	0.24	0.13
Cl	-7.11	-0.48	-0.44	0.69	0.20	-37257.42	0.23	-1258.28	-5.60	0.27	4.03	7.34	1.50	-16.82	0.19	0.13
Ar	-7.00	-0.49	-0.45	0.65	0.17	-42821.32	0.16	43.54	0.88	0.48	-0.16	0.50	1.38	-16.60	0.15	0.27
H_2	8.18	21.95	21.95	26.49	26.50	-4.50×10^{6}	24.99	425.18	21.62	18.30	21.49	25.40	22.85	-18.03	23.29	22.90
HF	-8.38	-0.22	-0.21	1.36	-0.02	-2.16×10^{5}	0.96	-21.84	0.82	0.53	-0.25	0.89	3.10	-23.91	0.70	0.54
LiH	-13.90	-3.67	-3.67	-1.17	-1.64	-50659.72	1.85	-39.12	-1.98	-2.67	-3.08	2.46	-1.54	-29.80	-2.67	-2.48
LiF	-10.06	-1.89	-1.88	-0.30	-1.59	-6.44×10^{5}	-0.51	-24.55	-0.80	-1.13	-1.91	-0.44	1.35	-25.49	-0.98	-1.13
N	-8.50	0.41	0.42	2.23	1.84	-4.24×10^{5}	2.47	-423.51	5.40	3.47	1.58	3.78	4.17	-25.36	1.44	1.71
H_2O	-8.44	0.05	0.06	1.74	0.93	-60724.44	1.32	37.25	0.09	1.62	-1.54	-0.03	3.60	-24.68	1.02	1.06
NH_3	-8.63	0.14	0.15	1.95	1.57	-32603.72	1.70	-105.76	5.32	2.92	1.41	3.82	3.80	-25.26	1.15	1.37
CH_4	-9.06	0.02	0.02	1.96	1.58	-28056.36	1.60	-60.39	3.08	1.79	0.62	1.99	3.63	-26.32	1.05	1.34

Table A.6: Percentage error of the kinetic energy of each functional with UHF/UGBS being the reference. Part 2.

Specie	$t_{\xi,B_{0/1,a}}$	$t_{\xi,B_{0/1j,a}}$	$t_{\xi,B_{0/1,b}}$	$t_{\xi,B_{0/1j,b}}$	$t_{\xi,B_{0/1,c}}$	$t_{\xi,B_{0/1j,c}}$	$t_{\xi,B_{0/1,d}}$	$t_{\xi,B_{0/1j,d}}$	$t_{\xi,B_{0/1,e}}$	$t_{\xi,B_{0/1j,e}}$	$t_{\xi,B_{0/1,f}}$	$t_{\xi,B_{0/1j,f}}$	$t_{\xi,B_{1/1,a}}$	$t_{\xi,B_{1/1j,a}}$
H_2	-428.71	12.84	10.09	8.18	16.56	10.49	-13.73	-47.29	20.98	9.58	16.42	-11.04	18.64	18.78
HF	-368.91	-0.29	-6.69	-8.38	-0.63	-6.59	-26.76	-54.43	0.33	-2.65	-3.71	91.99	-2.06	-1.78
LiH	-372.89	-8.44	-12.17	-13.91	-6.21	-10.91	-30.58	-56.96	-3.69	-10.10	-6.74	24.64	-6.13	-5.76
LiF	-364.73	-2.17	-8.38	-10.06	-2.42	-7.76	-28.06	-54.94	-1.37	-4.48	-5.37	-11.88	-3.75	-3.45
N_2	-373.29	-0.80	-6.70	-8.50	-0.43	-13.66	-26.51	-58.81	1.00	-3.83	-3.24	-13.02	-1.51	-0.51
H_2O	-254.38	-0.48	-6.70	-8.44	-0.56	-0.37	-26.67	-50.72	0.62	-3.19	-3.64	-65.05	-1.93	-1.24
NH_3	-360.29	-0.92	-6.86	-8.63	-0.66	-13.71	-26.70	-58.79	0.70	-3.84	-3.41	-16.34	-1.76	-0.79
CH_4	-372.01	-1.81	-7.28	-9.06	-1.03	-10.86	-26.92	-57.21	0.54	-4.79	-3.43	-8.29	-1.97	-1.19

Table A.7: Percentage error of the kinetic energy of each functional with UHF/UGBS being the reference. Part 3.

Specie	$t_{\xi,B_{1/1,b}}$	$t_{\xi,B_{1/1j,b}}$	$t_{\xi,B_{1/1,c}}$	$t_{\xi,B_{1/1j,c}}$	$t_{\xi,B_{1/1,d}}$	$t_{\xi,B_{1/1j,d}}$	$t_{\xi,B_{2/1,a}}$	$t_{\xi,B_{2/1,b}}$	$t_{\xi,B_{2/1,c}}$	$t_{MG_{1,a}}$	$t_{MG_{1,b}}$	$t_{MG_{1j,b}}$	$t_{MG_{2,a}}$	$t_{MG_{2j,a}}$
H_2	22.85	22.03	23.33	22.43	23.33	21.37	21.82	25.10	23.45	23.50	-223.77	-144.49	-12398.58	-779.86
HF	0.35	0.25	0.53	0.34	0.32	0.35	-0.19	1.34	0.55	3.11	-203.11	-147.48	-289.96	-60.53
LiH	-2.95	-2.73	-2.59	-2.79	-1.98	-3.00	-3.66	-1.35	-2.66	-1.27	-198.84	-143.96	-876.52	720.73
LiF	-1.32	-1.41	-1.13	-1.35	-1.35	-1.45	-1.86	-0.31	-1.12	1.37	-201.37	-146.54	-286.00	-34.36
N_2	1.06	0.96	1.28	1.10	1.84	6.20	0.52	2.21	1.24	4.17	-204.16	-140.18	-307.39	-35.95
H_2O	0.65	0.55	0.85	0.68	-0.84	0.65	0.02	1.72	0.90	3.60	-203.60	-143.68	-383.43	30.92
NH_3	0.77	0.61	0.99	0.80	1.52	4.17	0.24	1.91	0.96	3.81	-203.81	-140.51	-484.92	202.45
CH_4	0.68	0.60	0.92	0.72	1.09	2.72	0.09	1.91	0.92	3.65	-203.65	-146.64	-788.94	534.19

Table A.8: Percentage error of the kinetic energy of each functional with UPBEPBE/UGBS being the reference. Part 1.

Specie	t_0	$t_0 + t_2$	$t_0 + t_{2j}$	$t_0 + t_2 + t_4$	$t_0 + t_{2j} + t_{4j}$	$t_0 + t_2 + t_4 + t_6$	$t_{B_{0/1}}$	$t_{B_{0/1}\mathrm{j}}$	$t_{B_{1/1}}$	$t_{B_{1/1}\mathrm{j}}$	$t_{B_{2/1}}$	$t_{B_{1/2}}$	t_{MG_1}	$t_{MG_1\mathrm{j}}$	t_{MG_2}	$t_{MG_{2j}}$
H	-8.99	2.12	2.12	4.93	5.01	-539264.58	6.00	-108.70	1.12	2.57	-7.08	0.05	3.75	-26.33	3.24	2.45
He	-11.25	-0.13	-0.13	2.73	2.65	-53305506.51	-4.77	-210.85	-684.54	-0.33	5.68	4.04	2.08	-27.31	0.94	0.57
Li	-10.26	0.55	0.55	3.24	2.11	-28117786191.85	5.99	-35.81	2.72	1.62	0.82	6.37	2.80	-27.14	1.60	1.64
Be	-10.21	0.18	0.18	2.49	2.02	-4876.98	4.24	-122.59	-137.94	1.93	5.07	10.94	2.88	-27.47	1.24	1.27
B	-10.24	-0.28	-0.27	1.90	0.93	-18129.32	2.53	-40.28	1.62	1.25	0.26	3.25	2.81	-27.42	0.78	0.76
C	-9.91	-0.43	-0.42	1.59	1.18	-715167.99	2.02	-39.80	1.33	1.40	0.10	2.60	2.76	-26.88	0.61	0.93
N	-9.18	-0.18	-0.17	1.68	1.30	-1086172.49	1.53	-162.29	12.90	2.80	0.92	2.75	2.82	-25.01	0.80	1.03
O	-9.34	-0.74	-0.73	1.01	0.23	-1383880652.89	1.20	-147.87	-1.73	0.91	-2.59	-1.06	2.51	-24.98	0.21	0.40
F	-9.14	-0.94	-0.92	0.66	-0.72	-376209.42	0.33	-158.31	0.31	0.00	-0.99	0.29	2.29	-24.45	-0.04	-0.10
Ne	-8.55	-0.74	-0.73	0.73	-0.01	-403229.30	-0.78	282.78	5.40	0.37	0.54	0.73	2.26	-22.74	0.12	0.20
Na	-8.19	-0.63	-0.61	0.78	-0.49	-222206378.08	0.31	-43.06	0.21	0.25	-0.85	0.11	2.13	-21.40	0.19	0.21
Mg	-7.92	-0.56	-0.54	0.79	-0.44	-151.57	0.40	50.06	4.50	0.21	1.04	2.32	2.04	-20.99	0.22	0.08
Al	-7.72	-0.53	-0.50	0.78	-0.55	-717.90	0.33	-58.94	0.43	-0.14	-0.60	0.28	1.91	-19.66	0.23	0.21
Si	-7.54	-0.51	-0.48	0.75	-0.53	-1917.49	0.35	-18.55	-1.72	-0.14	-4.95	-2.95	1.79	-19.47	0.22	0.02
P	-7.37	-0.49	-0.46	0.74	0.21	-65126.73	0.29	3619.33	0.85	0.17	-0.16	0.63	1.68	-17.85	0.22	0.16
S	-7.27	-0.52	-0.49	0.68	0.16	34463.94	0.20	-67.87	0.07	0.87	-0.87	-0.14	1.54	-18.22	0.16	0.06
Cl	-7.17	-0.55	-0.51	0.62	0.13	-32626.45	0.17	167.32	-6.30	0.16	4.09	7.61	1.41	-16.62	0.12	0.05
Ar	-7.05	-0.56	-0.51	0.59	0.10	-33510.64	0.08	33.79	0.78	0.38	-0.22	0.43	1.30	-16.40	0.08	0.20
H_2	2.69	15.90	15.90	20.09	20.12	-1954322.64	13.32	-167.69	21.75	14.36	14.82	13.33	16.98	-22.59	17.17	16.60
HF	-8.71	-0.59	-0.58	0.98	-0.41	-144279.37	0.50	-24.42	0.91	0.42	-0.65	0.41	2.71	-24.05	0.32	0.15
LiH	-14.20	-3.97	-3.97	-1.56	-2.01	-7423.67	-1.14	-53.58	-2.34	-2.32	-3.72	-2.87	-1.62	-30.22	-2.97	-2.85
LiF	-10.23	-2.09	-2.07	-0.51	-1.81	-224.38	-0.49	-25.49	-0.90	-1.37	-2.12	-0.42	1.15	-25.54	-1.19	-1.36
N_2	-9.09	-0.26	-0.25	1.53	1.15	-329149.37	1.48	-116.45	4.13	2.73	0.88	2.73	3.51	-25.76	0.77	0.99
H_2O	-8.90	-0.47	-0.46	1.21	0.40	-58852.64	15.64	-38.24	-0.55	1.17	-2.15	-0.80	3.07	-24.90	0.49	0.51
NH_3	-9.15	-0.44	-0.44	1.34	0.96	-42197.22	1.22	-116.80	4.12	2.30	0.77	2.27	3.22	-25.56	0.55	0.72
CH_4	-9.56	-0.56	-0.55	1.35	0.97	-20489.35	1.49	-7.51	2.21	1.39	0.07	1.75	3.12	-26.67	0.46	0.71

Table A.9: Percentage error of the kinetic energy of each functional with UPBEPBE/UGBS being the reference. Part 2.

Specie	$t_{\xi,B_{0/1,a}}$	$t_{\xi,B_{0/1j,a}}$	$t_{\xi,B_{0/1,b}}$	$t_{\xi,B_{0/1j,b}}$	$t_{\xi,B_{0/1,c}}$	$t_{\xi,B_{0/1j,c}}$	$t_{\xi,B_{0/1,d}}$	$t_{\xi,B_{0/1j,d}}$	$t_{\xi,B_{0/1,e}}$	$t_{\xi,B_{0/1j,e}}$	$t_{\xi,B_{0/1,f}}$	$t_{\xi,B_{0/1j,f}}$	$t_{\xi,B_{1/1,a}}$	$t_{\xi,B_{1/1j,a}}$
H_2	-475.87	7.74	4.55	2.68	10.72	-0.93	-18.09	-51.99	15.81	4.46	48.11	4.60	12.65	12.74
HF	-367.05	-0.45	-7.02	-8.71	-0.91	-9.31	-27.03	-54.88	0.13	-2.79	-1.34	-7.26	-2.42	-2.13
LiH	-367.49	-8.27	-12.43	-14.20	-6.47	-13.50	-30.82	-57.27	-3.46	-10.08	-2.94	-8.16	-6.43	-6.01
LiF	-364.39	-2.13	-8.55	-10.23	-2.51	-10.20	-28.19	-55.24	-1.38	-4.44	-2.75	-11.42	-3.94	-3.65
N_2	-370.79	-1.13	-7.30	-9.09	-1.00	-16.66	-26.99	-59.40	0.57	-4.24	-0.69	-23.46	-2.17	-1.18
H_2O	-369.18	-0.73	-7.17	-8.90	-0.98	-3.44	-27.04	-51.28	0.29	-3.46	-0.91	-218.09	-2.44	-1.75
NH_3	-369.99	-1.16	-7.38	-9.15	-1.15	-16.51	-27.12	-59.27	0.35	-4.12	-1.48	-34.23	-2.34	-1.38
CH_4	-371.69	-1.93	-7.78	-9.56	-1.49	-13.60	-27.32	-57.59	0.26	-5.02	-0.73	-11.21	-2.54	-1.75

Table A.10: Percentage error of the kinetic energy of each functional with UPBEPBE/UGBS being the reference. Part 3.

Specie	$t_{\xi,B_{1/1,b}}$	$t_{\xi,B_{1/1j,b}}$	$t_{\xi,B_{1/1,c}}$	$t_{\xi,B_{1/1j,c}}$	$t_{\xi,B_{1/1,d}}$	$t_{\xi,B_{1/1j,d}}$	$t_{\xi,B_{2/1,a}}$	$t_{\xi,B_{2/1,b}}$	$t_{\xi,B_{2/1,c}}$	$t_{MG_{1,a}}$	$t_{MG_{1,b}}$	$t_{MG_{1j,b}}$	$t_{MG_{2,a}}$	$t_{MG_{2j,a}}$
H_2	16.95	15.78	17.23	16.60	16.95	15.30	15.72	18.97	17.38	17.58	-217.83	-144.34	-12435.73	-289.56
HF	0.10	-0.13	0.16	0.07	-0.07	1.22	-0.56	0.96	0.18	2.71	-202.71	-147.39	-326.27	-23.73
LiH	-3.10	-3.10	-2.89	-2.93	-3.34	-3.17	-3.95	-1.66	-2.93	-1.38	-198.73	-143.50	-773.14	3116.61
LiF	-1.40	-1.63	-1.34	-1.46	-1.54	-1.65	-2.07	-0.52	-1.31	1.16	-201.17	-146.70	-331.55	163.48
N_2	0.51	0.24	0.59	0.57	1.08	0.11	-0.16	1.51	0.56	3.51	-203.51	-143.61	-361.59	6.93
H_2O	0.25	0.00	0.32	0.29	-1.59	-0.26	-0.50	1.19	0.37	3.07	-203.07	-143.64	-400.74	98.67
NH_3	0.31	-0.03	0.39	0.34	0.52	-0.20	-0.35	1.31	0.38	3.23	-203.23	-142.41	-515.35	278.08
CH_4	0.23	-0.02	0.33	0.29	0.48	0.85	-0.49	1.31	0.35	3.13	-203.13	-146.42	-792.28	560.56

Bibliography

[1] Verstraelen, T. and Tecmer, P. and Heidar-Zadeh, F. and González-Espinoza, C. E. and Chan, M. and Kim, D. T. and Boguslawski, K. and Fias, S. and Vandenbrande, S. and Berrocal, D. and Ayers, P. W., "Horton: Helpful open-source research tool for n-fermion systems."

[2] E. Sim, J. Larkin, K. Burke, and C. W. Bock, "Testing the kinetic energy functional: Kinetic energy density as a density functional," *Journal of Chemical Physics*, vol. 118, no. 18, pp. 8140–8148, 2003.

[3] T. Hansson, C. Oostenbrink, and W. van Gunsteren, "Molecular dynamics simulations," *Current Opinion in Structural Biology*, vol. 12, no. 2, pp. 190 – 196, 2002.

[4] M. E. Tuckerman, "Ab initiomolecular dynamics: basic concepts, current trends and novel applications," *Journal of Physics: Condensed Matter*, vol. 14, pp. R1297–R1355, dec 2002.

[5] R. Car and M. Parrinello, "Unified approach for molecular dynamics and density-functional theory," *Phys. Rev. Lett.*, vol. 55, pp. 2471–2474, Nov

1985.

[6] K. Luo, V. V. Karasiev, and S. B. Trickey, "Towards accurate orbital-free simulations: A generalized gradient approximation for the noninteracting free energy density functional," *Physical Review B*, vol. 101, no. 7, pp. 1–9, 2020.

[7] D. R. Bowler, T. Miyazaki, and M. J. Gillan, "Recent progress in linear scalingab initioelectronic structure techniques," *Journal of Physics: Condensed Matter*, vol. 14, pp. 2781–2798, mar 2002.

[8] M. Pearson, E. Smargiassi, and P. A. Madden, "Ab initio molecular dynamics with an orbital-free density functional," *Journal of Physics: Condensed Matter*, vol. 5, pp. 3221–3240, may 1993.

[9] J. P. Perdew and K. Schmidt, "Jacob's ladder of density functional approximations for the exchange-correlation energy," *AIP Conference Proceedings*, vol. 577, no. 1, pp. 1–20, 2001.

[10] F. Tran and T. A. Wesolowski, "Semilocal Approximations for the Kinetic Energy," pp. 429–442, 2013.

[11] W. C. Witt, B. G. Del Rio, J. M. Dieterich, and E. A. Carter, "Orbital-free density functional theory for materials research," *Journal of Materials Research*, vol. 33, no. 7, pp. 777–795, 2018.

[12] Y. A. Wang, N. Govind, and E. A. Carter, "Orbital-free kinetic-energy density functionals with a density-dependent kernel," *Phys. Rev. B*, vol. 60, pp. 16350–16358, Dec 1999.

[13] E. H. Lieb and B. Simon, "The thomas-fermi theory of atoms, molecules and solids," *Advances in mathematics*, vol. 23, no. 1, pp. 22–116, 1977.

[14] L. H. Thomas, "The calculation of atomic fields," *Mathematical Proceedings of the Cambridge Philosophical Society*, vol. 23, no. 5, p. 542–548, 1927.

[15] E. Fermi, "Un metodo statistico per la determinazione di alcune priorieta dell'atome," *Rend. Accad. Naz. Lincei*, vol. 6, no. 602-607, p. 32, 1927.

[16] E. Teller, "On the stability of molecules in the thomas-fermi theory," *Rev. Mod. Phys.*, vol. 34, pp. 627–631, Oct 1962.

[17] D. Kirzhnits, "Quantum Corrections To the Thomas-Fermi Equation," *Soviet Phys. JETP*, vol. Vol: 5, 1957.

[18] C. H. Hodges, "Quantum Corrections to the Thomas–Fermi Approximation—The Kirzhnits Method," *Canadian Journal of Physics*, vol. 51, no. 13, pp. 1428–1437, 1973.

[19] D. R. Murphy, "Sixth-order term of the gradient expansion of the kinetic-energy density functional," *Physical Review A*, vol. 24, no. 4, pp. 1682–1688, 1981.

[20] M. Brack, B. K. Jennings, and Y. H. Chu, "= re(r)," vol. 65, no. 1, pp. 11–14, 1976.

[21] A. E. Mohammed, "Fourth-order gradient expansion of the fermion kinetic energy: Extra terms for nonanalytic densities," *Il Nuovo Cimento B (1971-1996)*, vol. 107, no. 4, pp. 375–383, 1992.

[22] Z. Yan, J. P. Perdew, T. Korhonen, and P. Ziesche, "Numerical test of the sixth-order gradient expansion for the kinetic energy:Application to the monovacancy in jellium," , vol. 55, pp. 4601–4604, June 1997.

[23] A. Sergeev, F. H. Alharbi, R. Jovanovic, and S. Kais, "Convergent sum of gradient expansion of the kinetic-energy density functional up to the sixth order term using Padé approximant," *Journal of Physics: Conference Series*, vol. 707, no. 1, 2016.

[24] A. Sergeev, R. Jovanovic, S. Kais, and F. H. Alharbi, "On the divergence of gradient expansions for kinetic energy functionals in the potential functional theory," *Journal of Physics A: Mathematical and Theoretical*, vol. 49, p. 285202, jun 2016.

[25] H. Mera, T. G. Pedersen, and B. K. Nikolić, "Nonperturbative quantum physics from low-order perturbation theory," *Phys. Rev. Lett.*, vol. 115, p. 143001, Sep 2015.

[26] H. Mera, T. G. Pedersen, and B. K. Nikolić, "Fast summation of divergent series and resurgent transseries from Meijer- G approximants," *Physical Review D*, vol. 97, no. 10, pp. 30–37, 2018.

[27] T. Helgaker, P. Jørgensen, and J. Olsen, *Perturbation Theory*, ch. 14, pp. 724–816. John Wiley Sons, Ltd, 2000.

[28] G. Arfken, m. Hans-Jürgen Weber, H. Weber, and F. Harris, *Mathematical Methods for Physicists*. Elsevier, 2005.

[29] K. F. Riley, M. P. Hobson, and S. J. Bence, *Mathematical Methods for Physics and Engineering: A Comprehensive Guide*. Cambridge University Press, 2 ed., 2002.

[30] E. Caliceti, M. Meyer-Hermann, P. Ribeca, A. Surzhykov, and U. D. Jentschura, "From useful algorithms for slowly convergent series to physical predictions based on divergent perturbative expansions," *Physics Reports*, vol. 446, no. 1-3, pp. 1–96, 2007.

[31] J. P. Boyd, "The Devil's Invention: Asymptotic, Superasymptotic and Hyperasymptotic Series," *Acta Applicandae Mathematicae*, vol. 56, no. 1, pp. 1–98, 1999.

[32] A. Najah, B. Cochelin, N. Damil, and M. Potier-Ferry, "A critical review of asymptotic numerical methods," *Archives of Computational Methods in Engineering*, vol. 5, no. 1, pp. 31–50, 1998.

[33] L. Zheng and X. Zhang, "Chapter 1 - introduction," in *Modeling and Analysis of Modern Fluid Problems* (L. Zheng and X. Zhang, eds.), Mathematics in Science and Engineering, pp. 1 – 37, Academic Press, 2017.

[34] "Chapter v the generalized hypergeometric function and the g-function," in *The Special Functions and Their Approximations* (Y. L. Luke, ed.), vol. 53 of *Mathematics in Science and Engineering*, pp. 136 – 208, Elsevier, 1969.

[35] K. Roach, "Meijer g function representations," in *Proceedings of the 1997 International Symposium on Symbolic and Algebraic Computation*, ISSAC '97, (New York, NY, USA), p. 205–211, Association for Computing Machinery, 1997.

[36] M. Marucho, "Non-borel summable 4 theory in zero dimension: A toy model for testing numerical and analytical methods," *Journal of Mathematical Physics*, vol. 49, no. 4, p. 043509, 2008.

[37] M. Beneke, "Large-order perturbation theory for a physical quantity," *Nuclear Physics, Section B*, vol. 405, no. 2-3, pp. 424–450, 1993.

[38] S. Sanders and M. Holthaus, "Hypergeometric continuation of divergent perturbation series. II. Comparison with Shanks transformation and Padé approximation," *arXiv*, 2018.

[39] P. Blanchard and E. Brüning, "Density functional theory of atoms and molecules," 2015.

[40] P. Hohenberg and W. Kohn, "Inhomogeneous electron gas," *Phys. Rev.*, vol. 136, pp. B864–B871, Nov 1964.

[41] P. A. Dirac, "Note on exchange phenomena in the thomas atom," in *Mathematical Proceedings of the Cambridge Philosophical Society*, vol. 26, pp. 376–385, Cambridge University Press, 1930.

[42] *The Electron Density as the Basic Variable: Early Attempts*, ch. 3, pp. 29–32. John Wiley Sons, Ltd, 2001.

[43] M. J. Frisch, G. W. Trucks, H. B. Schlegel, G. E. Scuseria, M. A. Robb, J. R. Cheeseman, G. Scalmani, V. Barone, G. A. Petersson, H. Nakatsuji, X. Li, M. Caricato, A. V. Marenich, J. Bloino, B. G. Janesko, R. Gomperts, B. Mennucci, H. P. Hratchian, J. V. Ortiz, A. F. Izmaylov, J. L. Sonnenberg, D. Williams-Young, F. Ding, F. Lipparini, F. Egidi, J. Goings, B. Peng, A. Petrone, T. Henderson, D. Ranasinghe, V. G. Zakrzewski, J. Gao, N. Rega, G. Zheng, W. Liang, M. Hada, M. Ehara, K. Toyota, R. Fukuda, J. Hasegawa, M. Ishida, T. Nakajima, Y. Honda, O. Kitao, H. Nakai, T. Vreven, K. Throssell, J. A. Montgomery, Jr., J. E. Peralta, F. Ogliaro, M. J. Bearpark, J. J. Heyd, E. N. Brothers, K. N. Kudin, V. N. Staroverov, T. A. Keith, R. Kobayashi, J. Normand, K. Raghavachari, A. P. Rendell, J. C. Burant, S. S. Iyengar, J. Tomasi, M. Cossi, J. M. Millam, M. Klene, C. Adamo, R. Cammi, J. W. Ochterski, R. L. Martin, K. Morokuma, O. Farkas, J. B. Foresman, and D. J. Fox, "Gaussian˜16 Revision C.01," 2016. Gaussian Inc. Wallingford CT.